V. HYDRODYNAMIC MODELING

V.1 INTRODUCTION

This section summarizes the field data collection effort and the development of a hydrodynamic model for the Three Bays estuary system in the Town of Barnstable. For this system, the final calibrated model offers an understanding of water movement through the estuary, and provides the first step towards evaluating water quality, as well as a tool for later determining nitrogen loading "thresholds". Nutrient loading data combined with measured environmental parameters within the system become the basis for an advanced water quality model based on total nitrogen concentrations. This type of model provides a tool for evaluating existing estuarine water quality parameters, as well as determining the likely positive impacts of various alternatives for improving overall estuarine health, facilitating the understanding how pollutant loadings into the estuary will affect the biochemical environment and its ability to sustain a healthy marine habitat.

In general, water quality studies of tidally influenced estuaries must include a thorough evaluation of the hydrodynamics of the estuarine system. Estuarine hydrodynamics control a variety of coastal processes including tidal flushing, pollutant dispersion, tidal currents, sedimentation, erosion, and water levels. Numerical models provide a cost-effective method for evaluating tidal hydrodynamics since they require limited data collection and may be utilized to numerically assess a range of management alternatives. Once the hydrodynamics of an estuary system are understood, computations regarding the related coastal processes become relatively straightforward extensions to the hydrodynamic modeling. For example, the spread of pollutants may be analyzed from tidal current information developed by the numerical models.

Coastal embayments like the Three Bays system are the initial recipients of freshwater flows (i.e., groundwater and surfacewater) and the nutrients they carry. An embayment's shape influences the time that nutrients are retained in them before being flushed out to adjacent open waters, and their shallow depths both decrease their ability to dilute nutrient (and pollutant) inputs and increase the secondary impacts of nutrients recycled from the sediments. Degradation of coastal waters and development are tied together through inputs of pollutants in runoff and groundwater flows, and to some extent through direct disturbance, i.e. boating, oil and chemical spills, and direct discharges from land and boats. Excess nutrients, especially nitrogen, promote phytoplankton blooms and the growth of epiphytes on eelgrass and attached algae, with adverse consequences including low oxygen, shading of submerged aquatic vegetation, and aesthetic problems.

A hydrodynamic study was performed for the Three Bays system, which is located on the south shore of Cape Cod. A section of a topographic map in Figure V-1 shows the general study area. The three Bays system has four major subdivisions, Cotuit Bay, West Bay, North Bay, and Prince's Cove. Cotuit Bay and West Bay both have there own outlets to Nantucket sound, and are connected though the Seapuit River and also via North Bay. Osterville Grand Island and Little Island lie within the Three Bays system. Dead Neck is the barrier island that describes the southern boundary of this estuarine system, and protects Grand Island from the open waters of Nantucket Sound.

Figure V-1. Topographic map detail of the Three Bays System, in Barnstable, Massachusetts.

The entire Three Bays system has a surface coverage of 1251 acres, including several small sub-embayments attached to the system's main sub-embayments. Cotuit Bay is the largest sub-embayment of the Three Bays system, covering 469 acres. The average depth of the whole embayment is 6.2 ft. West Bay has an area coverage of 343 acres and an average depth of 5.3 ft. North Bay has an area coverage of 309 acres, and an average depth of 5.3 ft. Prince's Cove together with Warren Cove and the Marstons Mills River are the northernmost reaches of the Three Bays system, with a 93-acre coverage. The Marstons Mills River is the largest surface source of fresh water into the estuary.

Circulation in the Three Bays system is dominated by tidal exchange with Nantucket Sound. There is negligible attenuation of the tide range throughout the system, even into its uppermost reaches in Prince's Cove. This indicates that there is little loss of tidal energy

through the system, either due to bottom friction in shallow areas or from channel restrictions, e.g., at the system inlets and the Little Island draw bridge.

This hydrodynamic study proceeded as two component efforts. In the first portion of the study, bathymetry, tide, and circulation velocity data were collected in order to accurately characterize the physical system, and to provide data necessary for the modeling portion of the study. The bathymetry survey of Three Bays was performed to determine the variation of embayment and channel depths throughout the system. This survey addressed the previous lack of available bathymetry data for this system. In addition to the survey, tides were recorded at seven locations within Three Bays for 44 days. These tide data were necessary to run and calibrate the hydrodynamic model of the system. Finally, an Acoustic Doppler Current Profiler (ADCP) survey was completed during a single tide cycle to measure ebb and flood velocities across five channel transects. The ADCP data were used to compute system flow rates and to provide an independent means of verifying the performance of the hydrodynamic model.

A numerical hydrodynamic model of the Three Bays system was developed in he second portion of this study. Using the bathymetry survey data, a model grid mesh was generated for use with the RMA-2 hydrodynamic code. The tide data from offshore Dead Neck were used to define the open boundary conditions that drive the circulation of the model at the two system inlets, and data from the five TDR stations within the system were used to calibrate and verify model performance to ensure that it accurately represents the dynamics of the real, physical system.

The calibrated computer model of Three Bays was used to compute the flushing rates of selected sub-embayments. Though water quality in an embayment cannot be directly inferred by use of computed flushing rates alone, they can serve as useful indicators of embayment flushing performance relative to other areas in the same system. The ultimate utility of this hydrodynamic model is as input into a constituent transport model, where water quality constituents like nitrogen are modeled to determine the real water quality dynamics of a system.

V.2 GEOMORPHIC AND ANTHROPOGENIC EFFECTS TO THE ESTUARINE SYSTEM

A general understanding of the hydrodynamic controls and coastal processes influencing estuarine dynamics provides the initial framework for the hydrodynamic analysis. In addition, both natural and anthropogenic changes to the estuarine system can guide the evaluation of effective alternatives to enhance tidal circulation and improve water quality.

The southern coast of Cape Cod between the Popponesset Bay and West Bay entrances can be considered a moderately dynamic region, where natural wave and tidal forces continue to reshape the shoreline. Due to the protection afforded by the islands of Marthas Vineyard and Nantucket, the south shore of Cape Cod is protected from the influence of long period open ocean wave conditions. Similar to many portions of the Massachusetts coast, the available sediment supply influences the migration and/or stability of tidal inlets. Tidal inlets can become overwhelmed by the gradual wave-driven migration of a barrier beach separating the estuaries from the ocean. In addition to these natural coastal processes, man-made structures often can influence the stability of a shoreline/tidal inlet system.

V.2.1 Natural Coastal Processes

For the Three Bays estuarine system, the process of barrier spit elongation continues to have a significant influence on tidal exchange. Over the past 80 years, the Sampsons Island barrier elongation has influenced tidal exchange through the Cotuit Bay entrance, where the

West Bay inlet has gradually become more vital to tidal exchange within the Three Bays system. Figure V-2 illustrates the gradual narrowing of the Cotuit Bay entrance since 1938. This narrowing has caused migration of the navigation channel to the west. By 2003, some coastal engineering structures along the west side of the inlet became undermined and collapsed into the channel. As the Sampsons Island spit continues to elongate, the Cotuit Bay entrance becomes narrower and the inlet becomes less efficient for tidal exchange.

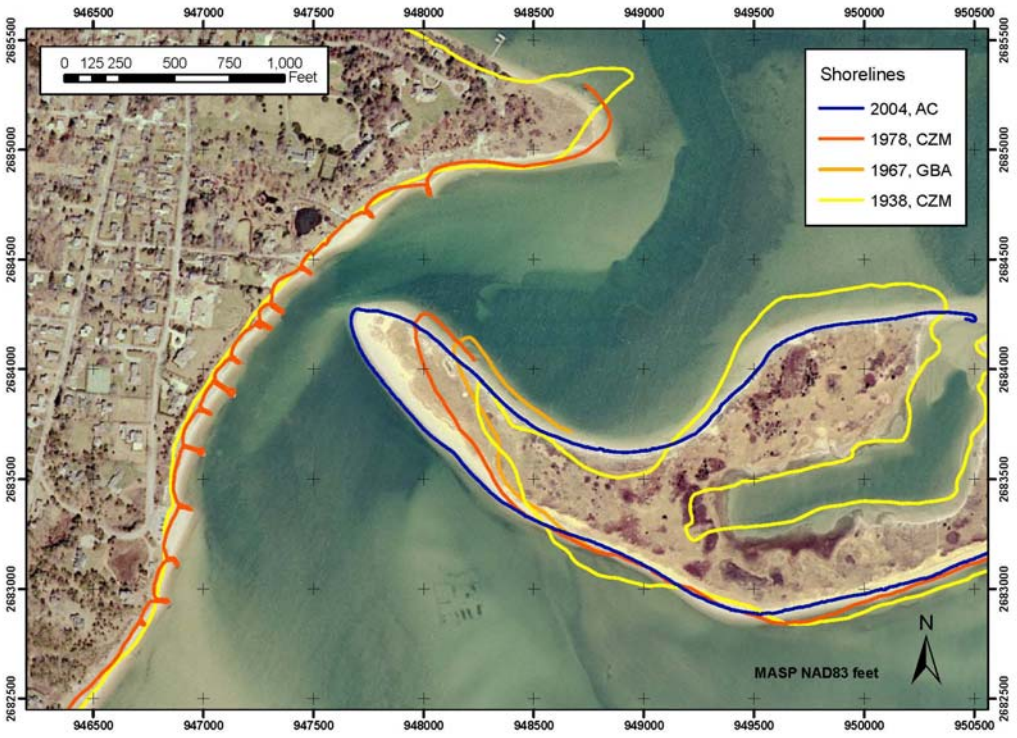

Figure V-2. Historical shoreline positions in the vicinity of the Cotuit Bay entrance between 1938 and 2004.

Figure V-3 shows the historic shoreline change fronting Rushy Marsh and the Three Bays region between 1938 and 2005. Much of the accretion along the barrier beach separating Rushy Marsh from Nantucket Sound is a result of the Popponesset spit remnants joining the barrier beach fronting Rushy Marsh. After this spit welded onto the existing shoreline, the net west-to-east directed littoral drift has "straightened" the shoreline in this region, where slight erosion has been observed along the beach fronting the southwest end of the pond and significant accretion has been observed along the beach fronting the remainder of the pond. To the northeast of Rush Marsh Pond, the shoreline has experienced erosion over the past 60+ years, likely resulting from the westerly migration of Sampsons Island.

Although littoral drift generally moves from west-to-east along the south shore of Cape Cod, due primarily to the prevailing southwest winds, a sediment transport reversal occurs along the shoreline of Dead Neck and Sampsons Islands. This local reversal is due to a slightly different shoreline orientation relative to the incident wave climate. As shown in Figure V-3, the east-to-west littoral drift generally causes erosion along the eastern portion of Dead Neck, with a corresponding accretion/spit elongation at the west end of Sampsons Island. The observed

erosion rates along the eastern portion of Dead Neck are moderated by ongoing beach nourishment efforts (described below).

Figure V-3. Observed shoreline change from 1938 to 2001/2005 for the shoreline area in the vicinity of Rushy Marsh Pond and Three Bays in Barnstable.

V.2.2 Anthropogenic Changes Influencing Rushy Marsh Pond

Manmade coastal structures along the shoreline immediately west of Cotuit Bay entrance consist primarily of groins along this updrift shoreline. Based on site observations, most of these structures are not effective barriers to natural littoral drift; therefore, beach compatible material continues to supply the beach systems along the shoreline of Cotuit Bay. The volume of material transported along this shoreline stretch is relatively small, due primarily to the quiescent wave conditions within the protected waters of Nantucket Sound. The conclusion that the longshore sediment transport rate is relatively low is further supported by the stable shoreline northeast of Rushy Marsh Pond and the small maintenance dredging volumes required to maintain the entrance to Cotuit Bay (which receives littoral sediments from both the east and the west).

The Three Bays estuarine system was significantly modified in 1900 by the construction of the West Bay cut. Prior to this time, only the Cotuit Bay entrance connected the Three Bays system to Nantucket Sound. Figure V-4 illustrates the condition of the system immediately before development of West Bay inlet. Creation of this structured inlet altered the tidal exchange within the Three Bays system, significantly reducing the volume of water flowing through the Cotuit Bay entrance.

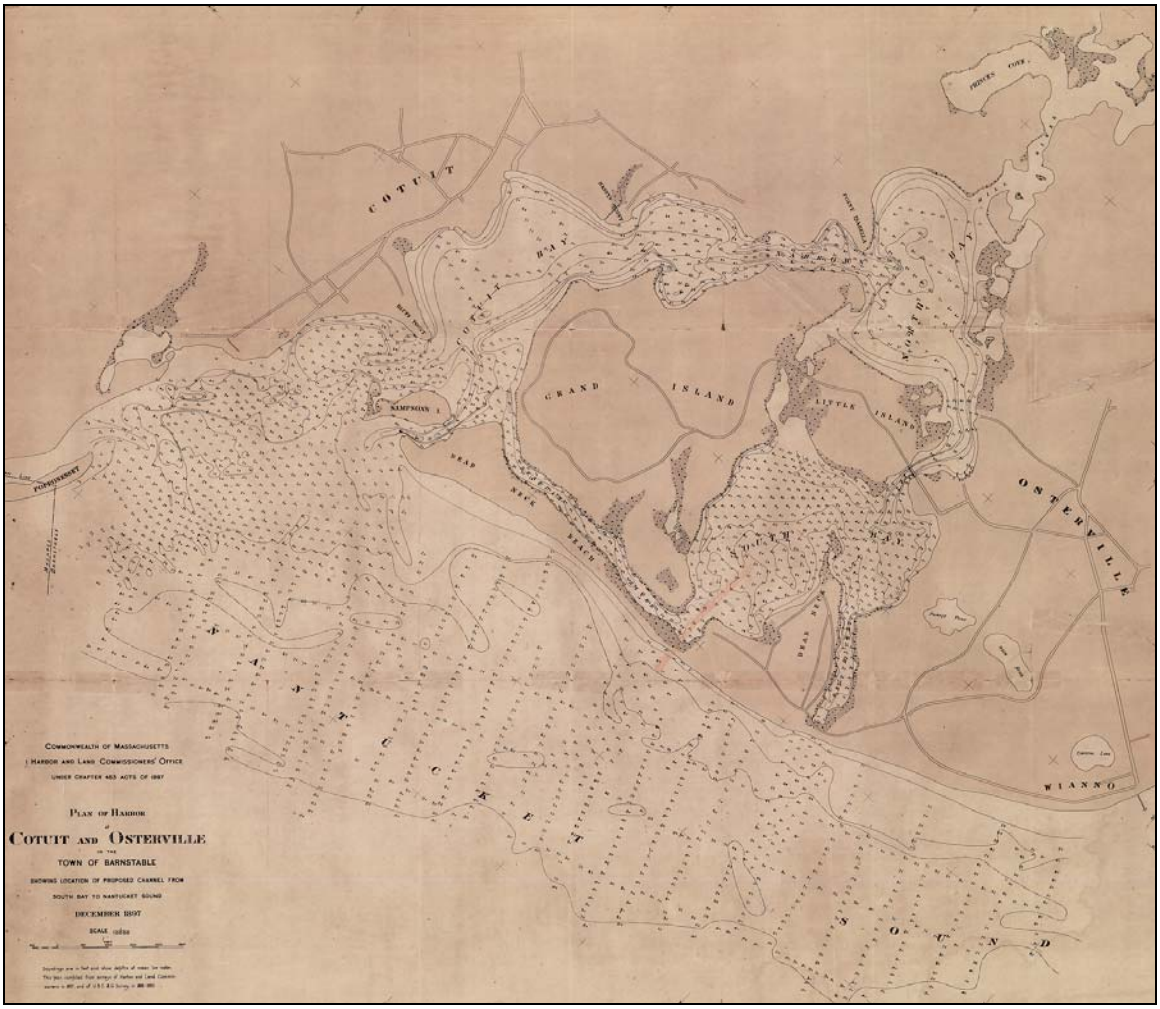

Figure V-4. Bathymetry map of the Three Bays estuarine system in 1897.

Over the past 20 years, significant efforts have been made by homeowners on Grand Island, as well as Three Bays Preservation, Inc. (a non-profit group concerned with the overall environmental conditions of Three Bays), to maintain the integrity of the Dead Neck barrier beach system. This maintenance of the barrier system has been in the form of beach nourishment as described below.

In order to enhance the storm protection capability of the eastern end of Dead Neck, two major beach nourishments have been completed on the island, adjacent to West Bay inlet. This segment of the Dead Neck shoreline has historically been the most erosive area of the island, due to it's proximity to West Bay inlet. The inlet, with its jetties, effectively interrupts littoral transport from updrift beaches. This has been the case since the opening of the inlet in the first half of the 20th century. Net transport along the Dead Neck shoreline is directed toward the Cotuit Bay entrance from the West Bay entrance. Therefore, as it is cut off from the natural source of sediment to the east, the east end of the island continues to erode (apparent as shoreline retreat and lowering of the island), further inhibiting its ability to adequately serve as storm protection for the area directly landward of the island (in the Seapuit River) and in West Bay.

For the first nourishment in 1985, 120,000 cubic yards of sand were placed along the section of beach starting at West Bay inlet and extending 2,400 feet westward (Wood, et al., 1996). Beach compatible material dredged from the West Bay inlet entrance channel was the source of sand used for this project. The design template of the nourishment had a berm elevation of +12.0 ft NGVD and a width of 100 ft. On average, the fill template required 50 to 60 cubic feet of sand per foot length of beach and had a stated design life of 10 years.

The performance of the 1985 nourishment was monitored on a semi-annual basis up to 1993. In 1993 approximately 7% of the nourishment volume remained in the template area. The average volume loss rate for the 7.5-year monitoring period was 14,880 cubic yards per year. Erosion rates along the template were higher than average at the completion of the nourishment as the beach fill profile equilibrated. Toward the end of the monitoring period, erosion rates were again accelerated due to a series of severe storms which impacted this shoreline during this time, including Hurricane Bob (August, 1991), the “no-name” northeast storm of October, 1991 and the Blizzard of 1993.

The second nourishment project commenced in the first half of 1999 and was completed in winter 2000 (Woods Hole Group, 2001). Figures V-5 and V-6 show the condition of the Dead Neck barrier beach in 1999 (immediately preceding nourishment) and 2000 (immediately following nourishment), respectively. The fill template for this nourishment had an elevation of +13 MLW, and a berm crest width of 150 feet. The sand used for the fill was available from channel maintenance dredging at Cotuit and West Bay Inlets. For this nourishment, 187,300 cubic yards were initially placed along a 2,000 foot-length of the Dead Neck shoreline, starting at the West Bay inlet. This resulted in an average fill volume of 95 cubic yards per foot of shoreline. In 2000, the fill was supplemented with an additional 25,100 cubic yards of sand, placed over the easternmost 1,000 feet of the island. The total volume of sand for the 1999-2000 nourishment project was therefore 212,400 cubic yards.

Since the completion of the nourishment in the first quarter of 2000, the movement of the Dead Neck shoreline has been monitored annually through the use of Differential GPS (DGPS) shoreline surveys and cross-shore profile measurements. These two data sets were used to determine shoreline change rates and volume loss in the 1999-2000 nourishment area, as well as shoreline change rates for the entire seaward shoreline of the island. In Figure V-7, measured shoreline change rates are indicated by color bars along the Dead Neck shoreline. For the whole seaward facing shoreline the maximum erosion rate was computed to be -23.4 feet per year (ft/yr). This maximum rate occurred about 1100 feet west of the West Bay Inlet. The average change rate over the 2,000 foot length of the 1999 nourishment was -17.0 feet during this period. At the western end of Dead Neck, the westernmost 1,000 feet of shoreline from Cotuit Inlet was accretional, with an average change rate of +4.9 ft/yr. Based on volume calculations, 36% of the fill volume has been lost from the nourishment area over the last five years. At the time of the September 2004 survey, there were 137,000 yd^3 of sand remaining. Over the approximate five-year period since the bulk of the 1999 nourishment was completed, the average rate of volume loss has been -13,700 yd^3/yr.

Figure V-5. The eastern portion of Dead Neck in 1999, showing at least two locations where the beach had significant storm overwash areas.

Figure V-6. Dead Neck Beach immediately following the beach nourishment in 2000, where the beach width had been increased significantly to prevent breaching of the barrier.

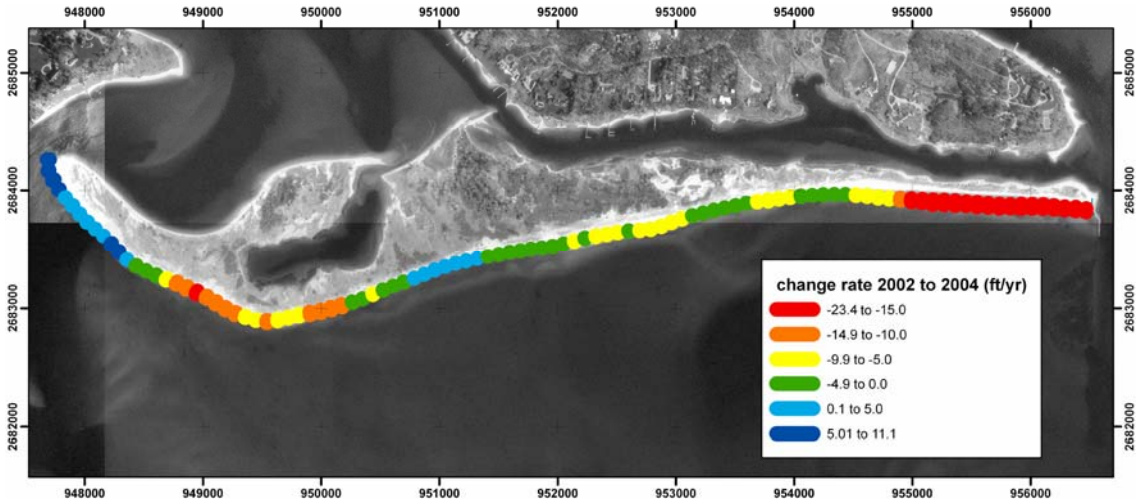

Figure V-7. Results of shoreline change analysis using the 2002 and 2004 GPS shorelines. Color bars indicate a range of shoreline change computed along Dead Neck. Negative rates indicate erosion, and are represented by the colors green, yellow, orange and red. Areas of accreting shoreline are indicated by light and dark blue.

V.3 DATA COLLECTION AND ANALYSIS

The field data collection portion of this study was performed to characterize the physical properties of the Three Bays estuary. Bathymetry were collected throughout the system so that it could be accurately represented as a computer hydrodynamic model, and so that flushing rates could be determined for the system sub-embayments. In addition to the bathymetry, tide data were also collected at seven locations, to run the circulation model with real tides, and also to calibrate and verify its performance.

V.3.1 Bathymetry Data Collection

Bathymetry data in Three Bays were collected during October 2002. Supplemental bathymetry were also available from a February 2002 survey of North and South Coves in Grand Island. The October 2002 survey employed a bottom tracking Acoustic Doppler Current Profiler (ADCP) mounted on a 12 ft motor skiff. Positioning data were collected using a differential GPS. The survey design included gridded transects at roughly 400 ft spacings in the main embayments, and finer spacings at the inlets. Survey paths are shown in Figure V-8. The resulting bathymetric surface created by interpolating the data to a finite element mesh is shown in Figure V-9. All bathymetry was tide corrected, and referenced to the National Geodetic Vertical Datum of 1929 (NGVD 29), using survey benchmarks located in the project area.

Results from the survey show that the deepest point in the Three Bays system is located at Cotuit Inlet, and is –23.6 ft NAVD. The greatest depths (approximately 15 ft) of Cotuit Bay are located in its southern portion, near the village of Cotuit. The greatest depths of West Bay are in the dredged navigation channel (approximately 10 ft) from the West Bay inlet to the entrance to North Bay. The deepest depths of the entire Three Bays system (apart from the inlets) are located in North Bay (approximately 17 ft) near its entrance to Cotuit Bay.

V.3.2 Tide Data Collection and Analysis

Tide data records were collected at seven stations in the Three Bays estuary: 1) offshore Dead Neck, 2) West Bay (Grand Island), 3) Cotuit Bay (Bluff Point), 4) North Bay (Oyster Harbors Marina), 5) North Bay (Point Isabella), 6) Dam Pond, and 7) Prince's Cove. An eighth tide gauge had been deployed in Cotuit Bay of off Handy Point, but data were not recovered from this location due to failure of the gauge. The locations of the stations are shown in Figure V-8. The Temperature Depth Recorders (TDR) used to record the tide data were deployed for a 44-day period between October 2, 2002 and November 15, 2002. The elevation of each gauge was surveyed relative to NGVD 29. Two gauges were deployed together offshore Dead Neck by SCUBA divers using a screw anchor. Duplicate offshore gauges were deployed to ensure data recovery, since the offshore tide record is crucial for developing the open boundary condition of the hydrodynamic model of the Three Bays system. Data from the other six locations were used to calibrate the model.

Plots of the tide data from three representative gauges are shown in Figure V-10, for the entire 44-day deployment. The spring-to-neap variation in tide can be seen in these plots. From the plot of the data from offshore Dead Neck, the tide reaches its maximum spring tide range of approximately 4.0 feet around October 7, and about seven days later the neap tide range is much smaller, as small as 1.5 feet. The second spring tide should occur around October 21, but the tide range is not clearly larger than either seven days before or after this date. The largest spring tide range is expected to occur at the time of the new moon, which occurred October 6 and again on November 4. The muted spring tide of October 21 occurred during the full moon. The causes of this odd feature of the tide in this are discussed from the results of the harmonic analysis later in this section.

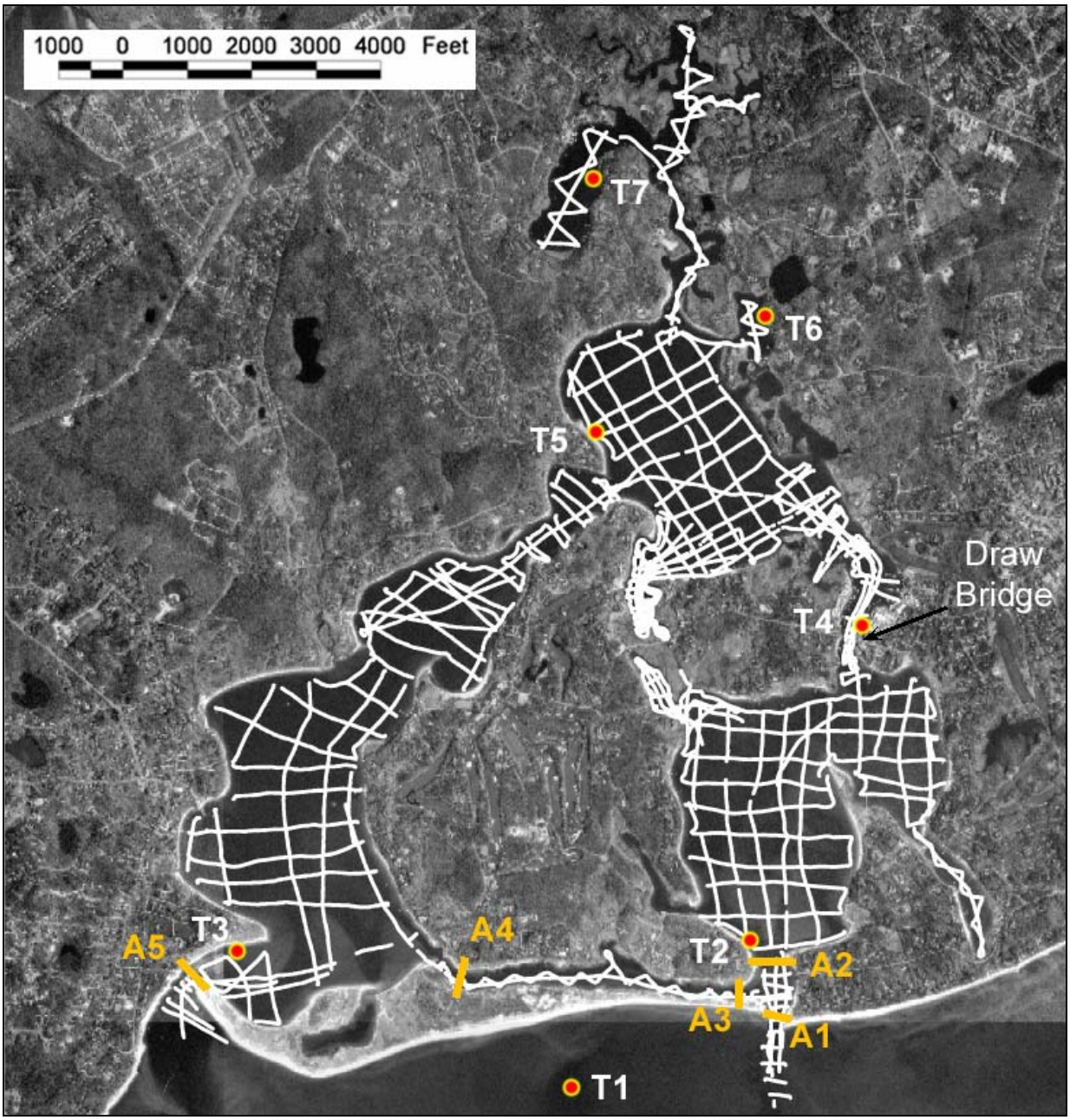

Figure V-8. Transects from the bathymetry survey of the Three Bays system. Red markers show the locations of the seven tide recorders deployed for this study.

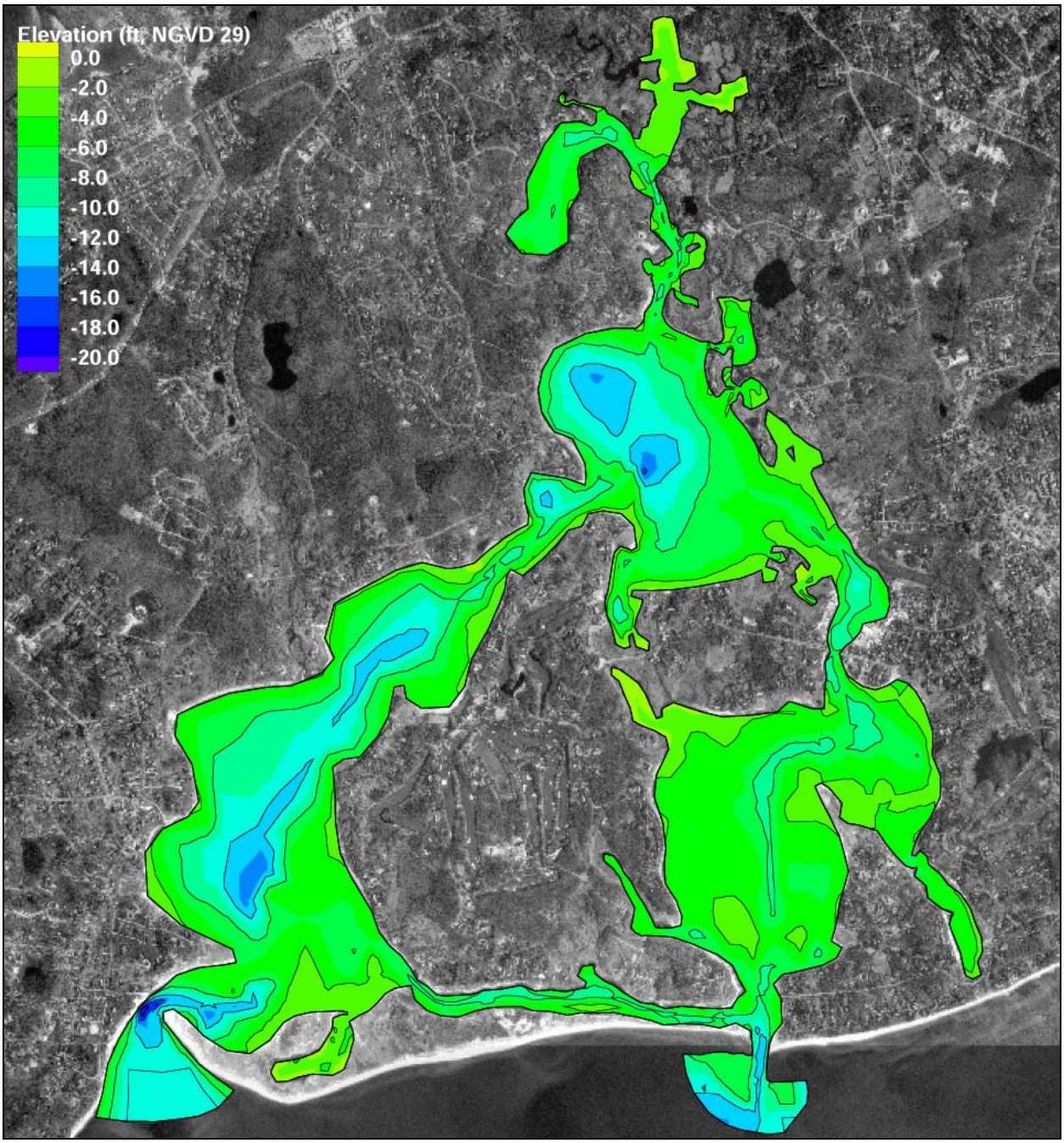

Figure V-9. Plot of interpolated finite-element grid bathymetry of the Three Bays system, shown superimposed on 1994 aerial photos of the system locale. Bathymetric contours are shown in color at two-foot intervals, and also as lines at four-foot intervals.

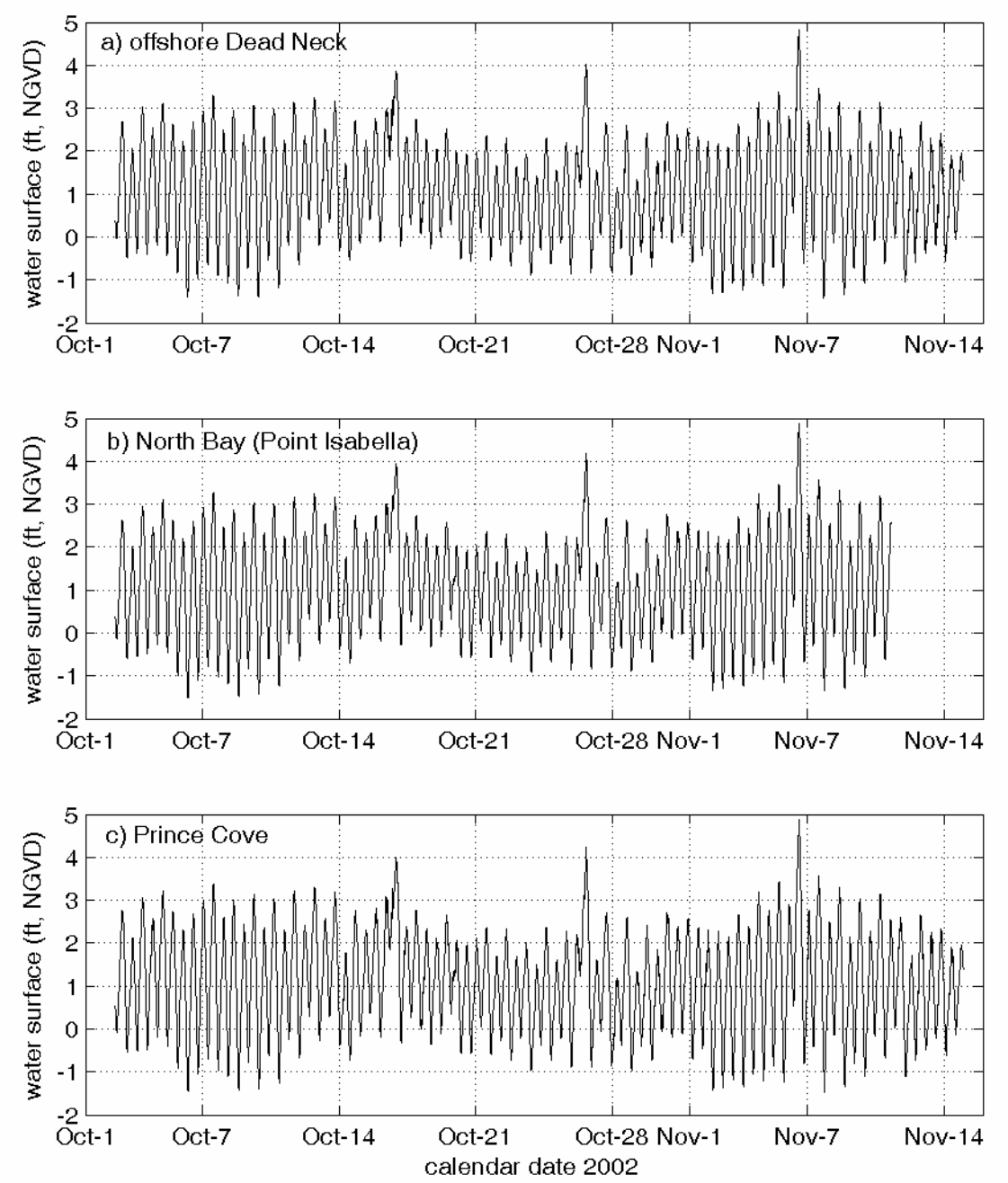

Figure V-10. Plots of observed tides for the Three Bays system, for the 44-day period between October 2 and November 15, 2002. The top plot shows tides offshore Dead Neck, in Nantucket Sound. The middle plot shows tides recorded in North Bay at Point Isabella, and the bottom plot shows tides recorded at Prince's Cove, in the upper reaches of the Three Bays system. All water levels are referenced to the National Geodetic Vertical Datum of 1929 (NGVD 29).

Also seen in this record are three distinct storm events, with peak storm surge levels occurring October 16, October 26, and November 6. Though the water level at peak surge is not substantially higher than the apparent normal peak spring tide levels, these surges stand out because of the relatively small tide range in this area of Nantucket Sound.

A visual comparison in Figure V-11 between tide elevations at the three stations shows that there negligible reduction in the tide range in the upper reaches of the Three Bays system. The loss of amplitude with distance from the inlet is described as tidal attenuation. Frictional mechanisms dissipate tidal flow energy, resulting in a reduction of the height of the tide. Tide attenuation is accompanied by a time delay (or phase lag) in the time of high and low tide (relative to the offshore tide), which becomes more pronounced farther into an estuary. The tide lag greatest in Prince's Cove, as seen in Figure V-10, where low tide in this sub-embayment occurs approximately 50 minutes after low tide in Nantucket Sound.

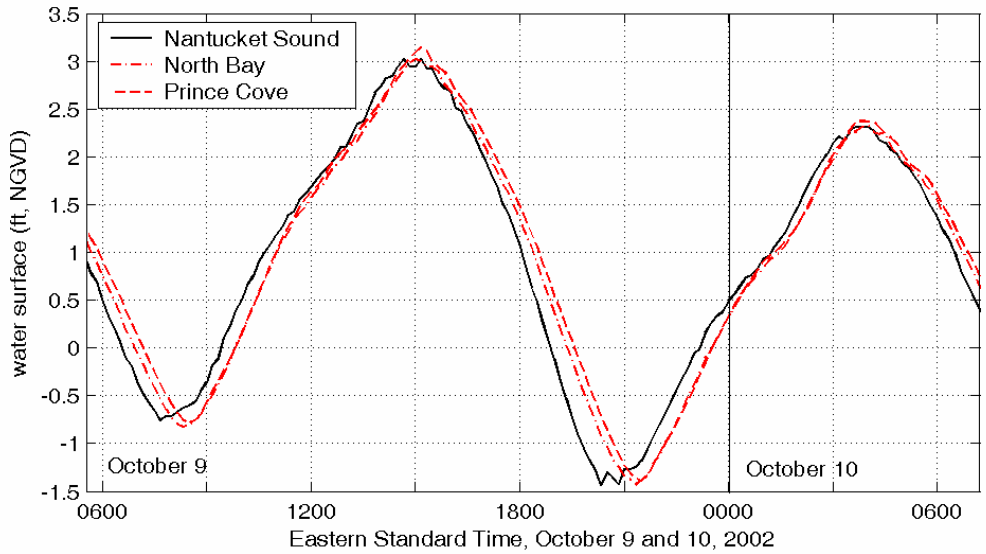

Figure V-11. Plot showing two tide cycles tides at three stations in the Three Bays system plotted together. Demonstrated in this plot is the minor frictional damping effect caused by flow restrictions at the inlets. The damping effects are seen only as a lag in time of high and low tides from Nantucket Sound. The time lag of low tide between the Sound and Prince's Cove in this plot is 50 Minutes.

Standard tide datums were computed from the 44-day records. These datums are presented in Table V-1. For most NOAA tide stations, these datums are computed using 19 years of tide data, the definition of a tidal epoch. For this study, a significantly shorter time span of data was available, however, these datums still provide a useful comparison of tidal dynamics within the system. The Mean Higher High (MHH) and Mean Lower Low (MLL) levels represent the mean of the daily highest and lowest water levels. The Mean High Water (MHW) and Mean Low Water (MLW) levels represent the mean of all the high and low tides of a record, respectively. The Mean Tide Level (MTL) is simply the mean of MHW and MLW. The lack of tide attenuation through the Three Bays estuary is apparent by how there is essentially no change in the elevation of each of the datums, from Nantucket Sound to Prince's Cove. This is true for even the maximum and minimum tide levels.

Table V-1. Tide datums computed from 44-day records collected offshore Dead Neck and in Cotuit Bay, West Bay, and Prince's Cove. Datum elevations are given relative to NGVD 29.

Tide Datum	Offshore	Cotuit Bay	West Bay	Prince's Cove
Maximum Tide	4.8	4.8	4.7	4.9
MHHW	2.8	2.8	2.8	2.9
MHW	2.4	2.4	2.4	2.4
MTL	1.0	1.0	1.0	1.0
MLW	-0.4	-0.4	-0.4	-0.5
MLLW	-0.7	-0.7	-0.7	-0.8
Minimum Tide	-1.4	-1.5	-1.4	-1.6

The tides in Nantucket Sound are semi-diurnal, meaning that there are typically two tide cycles in a day. There is usually a small variation in the level of the two daily tides. This variation can be seen in the differences between the MHHW and MHW, as well as the MLLW and MLW levels.

A more thorough harmonic analysis of the tidal time series was performed to produce tidal amplitude and phase of the major tidal constituents, and provide assessments of hydrodynamic 'efficiency' of the system in terms of tidal attenuation. This analysis also yielded a quantitative assessment of the relative influence of non-tidal, or residual, processes (such as wind forcing) on the hydrodynamic characteristics of each system.

A harmonic analysis was performed on the time series from each gauge location. Harmonic analysis is a mathematical procedure that fits sinusoidal functions of known frequency to the measured signal. The observed astronomical tide is therefore the sum of several individual tidal constituents, with a particular amplitude and frequency. For demonstration purposes a graphical example of how these constituents add together is shown in Figure V-12. The amplitudes and phase of 23 known tidal constituents result from this procedure. Table V-2 presents the amplitudes of eight tidal constituents in the Three Bays system.

The M_2, or the familiar twice-a-day lunar semi-diurnal tide, is the strongest contributor to the signal with an amplitude of 1.2 ft throughout the system. The total range of the M_2 tide is twice the amplitude, or 2.4 ft. The M_4 and M_6 tides are higher frequency harmonics of the M_2 lunar tide (exactly half the period of the M_2 for the M_4, and one third of the M_2 period for the M_6), results from frictional attenuation of the M_2 tide in shallow water. The M_4 has an amplitude of 0.2 feet in all sub-embayments of the system. The M_6 has a very small amplitude in the system (less than 0.1 feet). There is no change in the M_2 or its harmonics through the estuary, which is a further indication that friction losses in the system are minimal, and that Three Bays flushes effectively, even to its farthest reaches at Prince's Cove.

The other major tide constituents also show little variation across the system. The diurnal tides (once daily), K_1 and O_1, possess equal amplitudes of approximately 0.4 feet. Other semi-diurnal tides, the S_2 (12.00 hour period) and N_2 (12.66-hour period) tides, contribute significantly to the total tide signal, with amplitudes of 0.2 feet and 0.4 feet, respectively. The M_{sf} is a lunarsolar fortnightly constituent with a period of approximately 14 days, and is the result of the periodic conjunction of the sun and moon, and has an amplitude less than 0.1 ft.

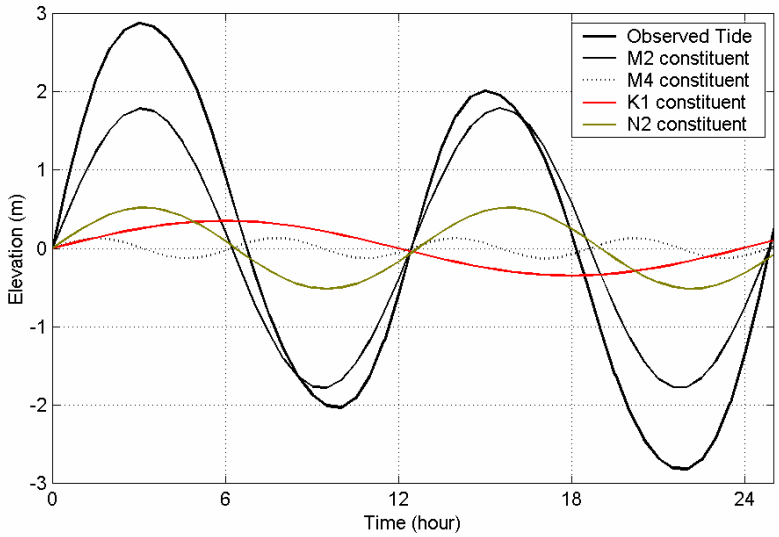

Figure V-12. Example of an observed astronomical tide as the sum of its primary constituents.

Table V-2. Major tidal constituents determined for gauge locations in Three Bays, October 2 through November 14, 2002.

	Amplitude (feet)							
Constituent	M2	M4	M6	S2	N2	K1	O1	Msf
Period (hours)	12.42	6.21	4.14	12.00	12.66	23.93	25.82	354.61
Nantucket Sound	1.20	0.17	0.07	0.15	0.41	0.35	0.35	0.06
Cotuit Bay	1.19	0.15	0.06	0.14	0.42	0.35	0.35	0.05
West Bay	1.20	0.15	0.07	0.15	0.41	0.35	0.35	0.06
Oyster Harbor Marine	1.20	0.14	0.08	0.15	0.41	0.35	0.35	0.05
North Bay	1.19	0.14	0.09	0.15	0.41	0.35	0.35	0.09
Dam Pond	1.17	0.14	0.08	0.14	0.40	0.35	0.35	0.05
Prince's Cove	1.20	0.14	0.09	0.15	0.41	0.35	0.35	0.05

Though there is no change in constituent amplitudes, the phase change of the tide is easily seen from the results of the harmonic analysis. Table V-3 shows the delay of the M_2 at different points in the Three Bays system, relative to the timing of the M_2 constituent in Nantucket Sound, offshore Dead Neck. The greatest delay is at the Dam Pond TDR station, which also showed the largest reduction of the M_2 amplitude (Table V-2). Compared to other locations instrumented in this study, Dam Pond shows the greatest tidal attenuation.

Table V-3. M_2 tidal constituent phase delay (relative to Nantucket Sound) for gauge locations in the Three Bay system, determine from measured tide data.

Station	Delay (minutes)
Cotuit Bay (Bluff Point)	7.1
West Bay	10.1
Oyster Harbor Marine (Draw Bridge)	15.3
North Bay (Point Isabella)	12.0
Dam Pond	23.1
Prince's Cove	20.5

Results of the harmonic analysis provide the reason why the transition from spring to neap tide ranges is not as apparent, as it is at other areas (e.g., Cape Cod Bay), as discussed earlier. The cause of the mute transition between spring and neap tide ranges is the relatively large amplitudes of the N_2 (larger lunar elliptic semidiurnal constituent) and O_1 (lunar diurnal constituent) constituents. From the analysis of other tide records from around southeastern Massachusetts, the N_2 has a typical amplitude that is less than 10% of the total tide, and the O_1 is typically less than 7% of the total tide amplitude. At Three Bays however, the N_2 and O_1 have much larger amplitudes relative to the total tide, at 15% and 13%, respectively. These constituents are slightly out of phase with the M_2 and K_1 (normally the greater contributors to the total tide amplitude), and therefore add and subtract from the total observed tide signal in cycles that are different (longer) than the 7 lunar day transition from spring to neap tides. In other areas (again, like Cape Cod Bay), the N_2 and O_1 represent a smaller percentage of the total observed tide, so their effect on the observed tide would be smaller.

In addition to the tidal analysis, the data were further evaluated to determine the importance of tidal versus non-tidal processes to changes in water surface elevation. These other processes include wind forcing (set-up or set-down) within the estuary, as well as sub-tidal oscillations of the sea surface. Variations in water surface elevation can also be affected by freshwater discharge into the system, if these volumes are relatively large compared to tidal flow. The results of an analysis to determine the energy distribution (or variance) of the original water elevation time series for the Three Bays system is presented in Table V-4 compared to the energy content of the astronomical tidal signal (re-created by summing the contributions from the 23 constituents determined by the harmonic analysis). Subtracting the tidal signal from the original elevation time series resulted with the non-tidal, or residual, portion of the water elevation changes. The energy of this non-tidal signal is compared to the tidal signal, and yields a quantitative measure of how important these non-tidal physical processes can be to hydrodynamic circulation within the estuary. Figure V-13 shows the comparison of the measured tide from Nantucket Sound, with the computed astronomical tide resulting from the harmonic analysis, and the resulting non-tidal residual.

Table V-4. Percentages of Tidal versus Non-Tidal Energy for Three Bays embayments, August to September 2001.

TDR LOCATION	Total Variance (ft^2)	Tidal (%)	Non-tidal (%)
Nantucket Sound (offshore)	1.048	86.9	13.1
Cotuit Bay (Bluff Point)	1.031	85.5	14.5
West Bay	1.035	86.6	13.4
Oyster Harbor Marina (North Bay)	1.042	86.3	13.7
North Bay (Point Isabella)	1.070	85.7	14.3
Dam Pond	1.001	85.8	14.2
Prince's Cove	1.042	85.9	14.1

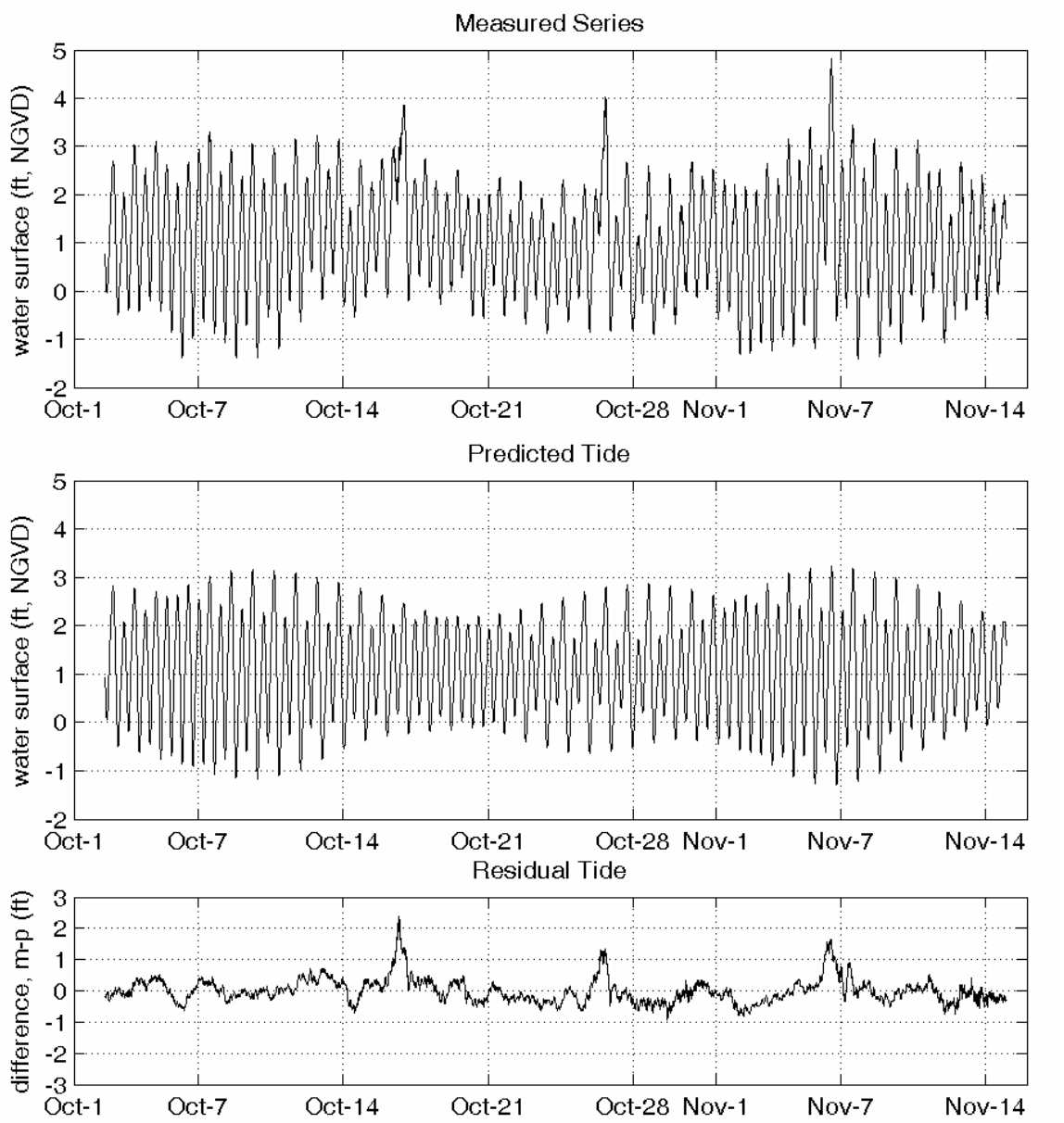

Figure V-13. Plot showing the comparison between the measured tide time series (top plot), and the predicted astronomical tide (middle plot) computed using the 23 individual tide constituents determine in the harmonic analysis of the Nantucket Sound (offshore Dead Neck) gauge data. The residual tide shown in the bottom plot is computed as the difference between the measured and predicted time series (r=m-p).

Table V-4 shows that the variance of tidal energy was essentially equal in all parts of the system; as should be expected given the minimal tidal attenuation through the system. The analysis also shows that tides are responsible for approximately 86% of the water level changes in Three Bays system. The remaining 14% was the result of atmospheric forcing, due to winds, or barometric pressure gradients. The largest tide residuals occurred at the three dates discussed earlier, October 16, October 26 and November 6. These are storm-induced surges caused by low pressure fronts moving through the area at those times, as indicated in regional meteorological data records.

V.3.3 ADCP Data Analysis

Cross-channel current measurements were surveyed through a complete tidal cycle in the Three Bays system on October 24, 2002 to resolve spatial and temporal variations in tidal current patterns. The survey was designed to observe tidal flow across five transects in the system at hourly intervals. These transects (indicated in Figure V-8) were located at the two system inlets, in the Seapuit River, as well as the entrance to West Bay, north of the eastern end of the Seapuit River. The data collected during this survey provided information that was necessary to model properly the hydrodynamics of the Three Bays system.

Figures V-15 through V-23 show color contours of the current measurements observed during the flood and ebb tides at each of the three transects. Positive along-channel currents (top panel) indicate the flow is moving into the estuary, while positive cross-channel velocities (middle panel) are oriented 90° clockwise of positive along-channel. For example, at West Bay inlet, positive along-channel flow is to the north, and positive cross-channel flow is moving to east. In Figure V-14, the lower left panel shows depth-averaged currents across the channel projected onto a 1994 aerial photograph of the inlet. The lower right panel of each figure indicates the stage of the tide that the survey transect was taken by a vertical line through the water elevation curve.

At the inlets, maximum measured currents in the water column were between 2.5 and 3.0 ft/sec (1.5 and 1.8 knots), with the larger velocities occurring at West Bay inlet. Flow rates (computed using the ADCP velocity data) through both inlets were roughly the same during the measured tide cycle. Maximum flood flows in the morning of the October 24 were 3000 ft^3/sec at West Bay inlet, and 3200 ft^3/sec at Cotuit Bay inlet. In the afternoon, maximum ebb flows were 3500 ft^3/sec and 4700 ft^3/sec at West Bay inlet and Cotuit Bay inlet, respectively.

The ADCP data from the two Seapuit River transects were critical for the determination of the direction and magnitude of tidal flows within the river. The data show that as the tide floods into Cotuit Bay and West Bay inlets, the river flows from east to west. During the ebb stage of the tide, the flow direction in the river reverses, flowing to the east. Further analysis (Section 3) shows that the flow through the Seapuit River is driven by a slight difference in the timing of the stage of the tide between West Bay inlet and Cotuit Bay inlet.

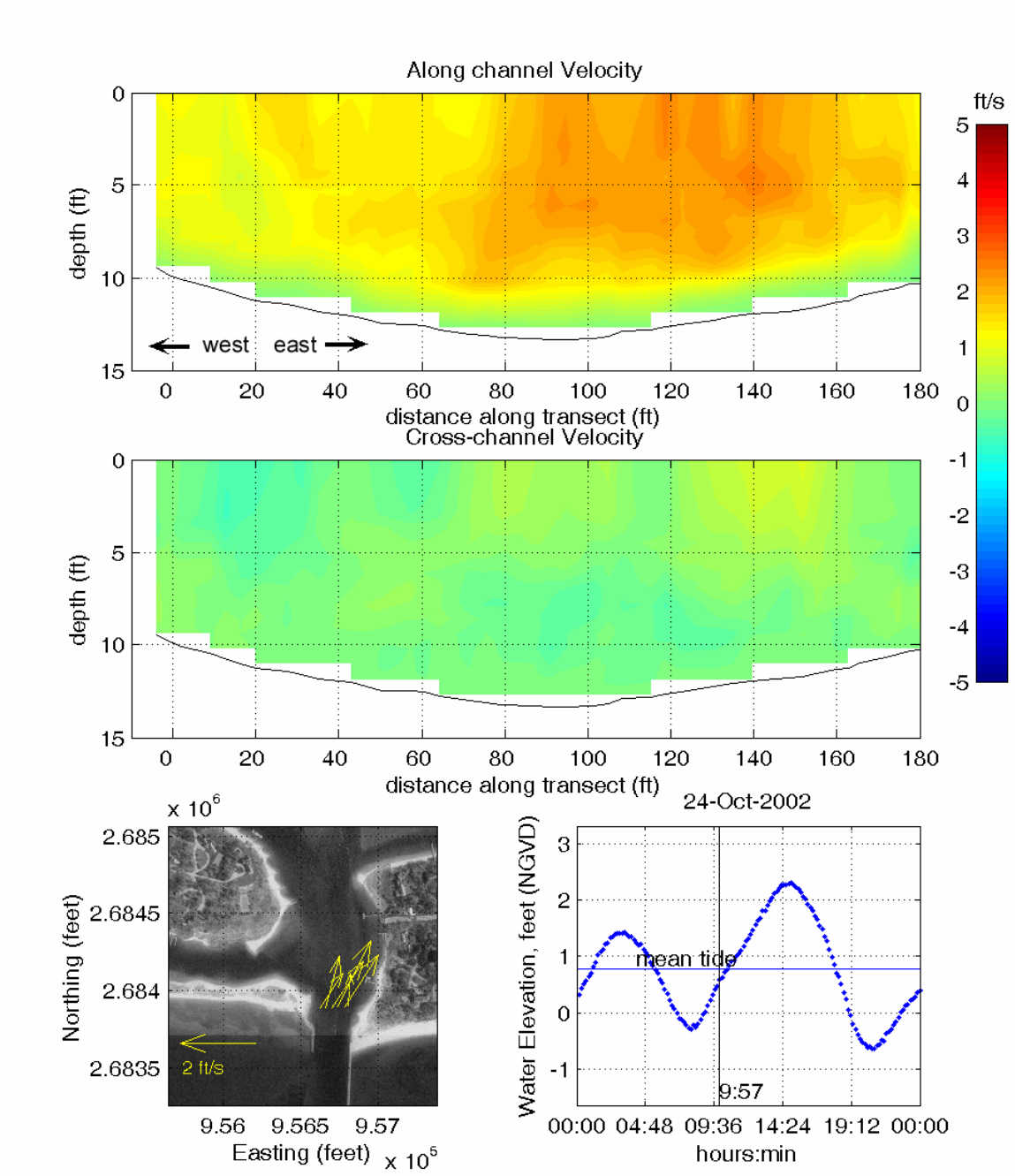

Figure V-14. Color contour plots of along-channel and cross-channel velocity components for transect line run east-to-west across West Bay inlet measured at 9:57 on October 24, 2001 during the period of maximum flood tide currents. Positive along-channel currents (top panel) indicate the flow is moving into the estuary, while positive cross-channel velocities (middle panel) are oriented 90° clockwise of positive along-channel. Lower left plot shows scaled velocity vectors projected onto a 1994 aerial photo of the survey area. A tide plot for the survey day is also given.

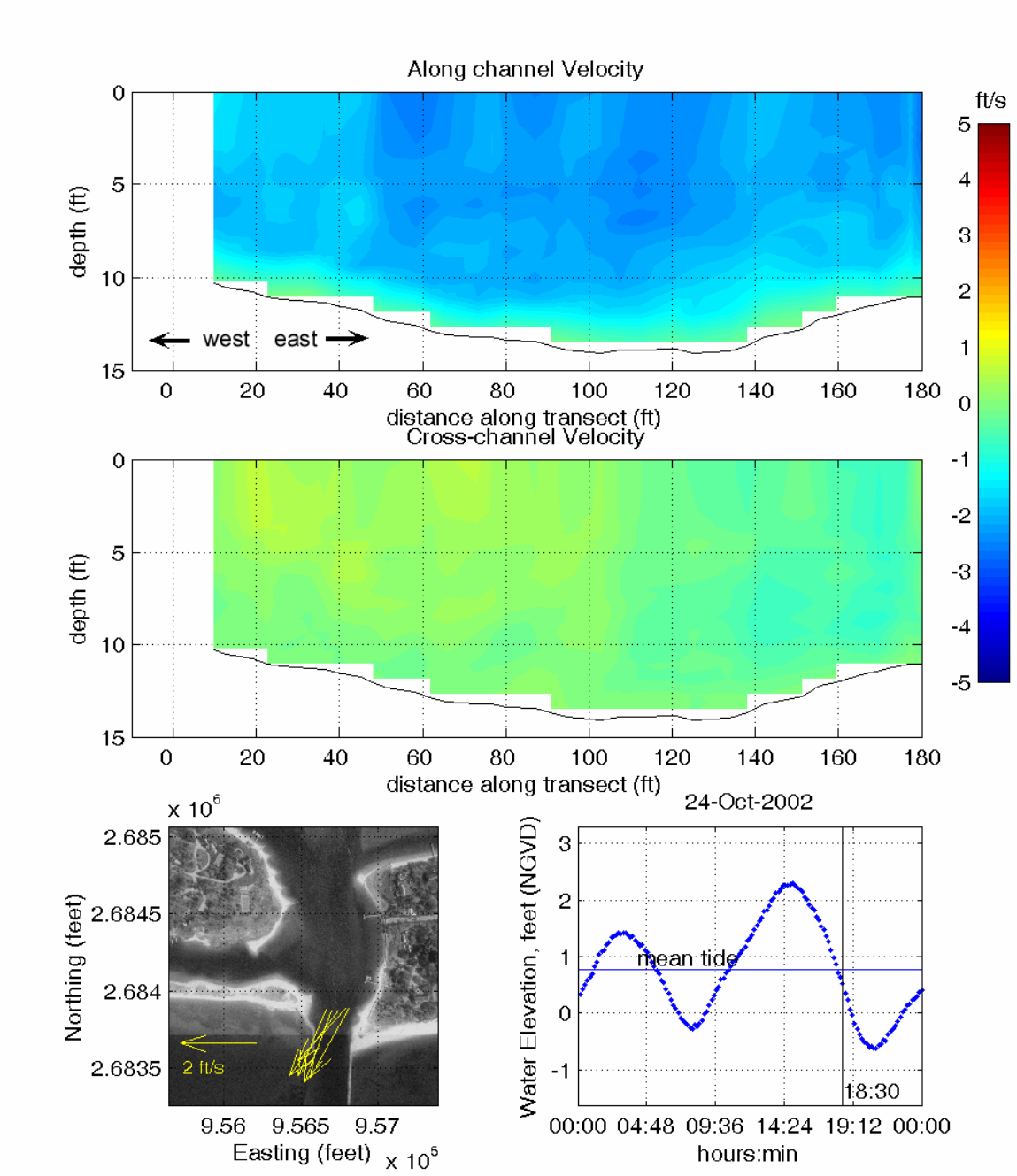

Figure V-15. Color contour plots of along-channel and cross-channel velocity components for transect line run east-to-west across West Bay inlet measured at 18:30 on October 24, 2001 during the period of maximum ebb tide currents. Positive along-channel currents (top panel) indicate the flow is moving into the estuary, while positive cross-channel velocities (middle panel) are oriented 90° clockwise of positive along-channel. Lower left plot shows scaled velocity vectors projected onto a 1994 aerial photo of the survey area. A tide plot for the survey day is also given.

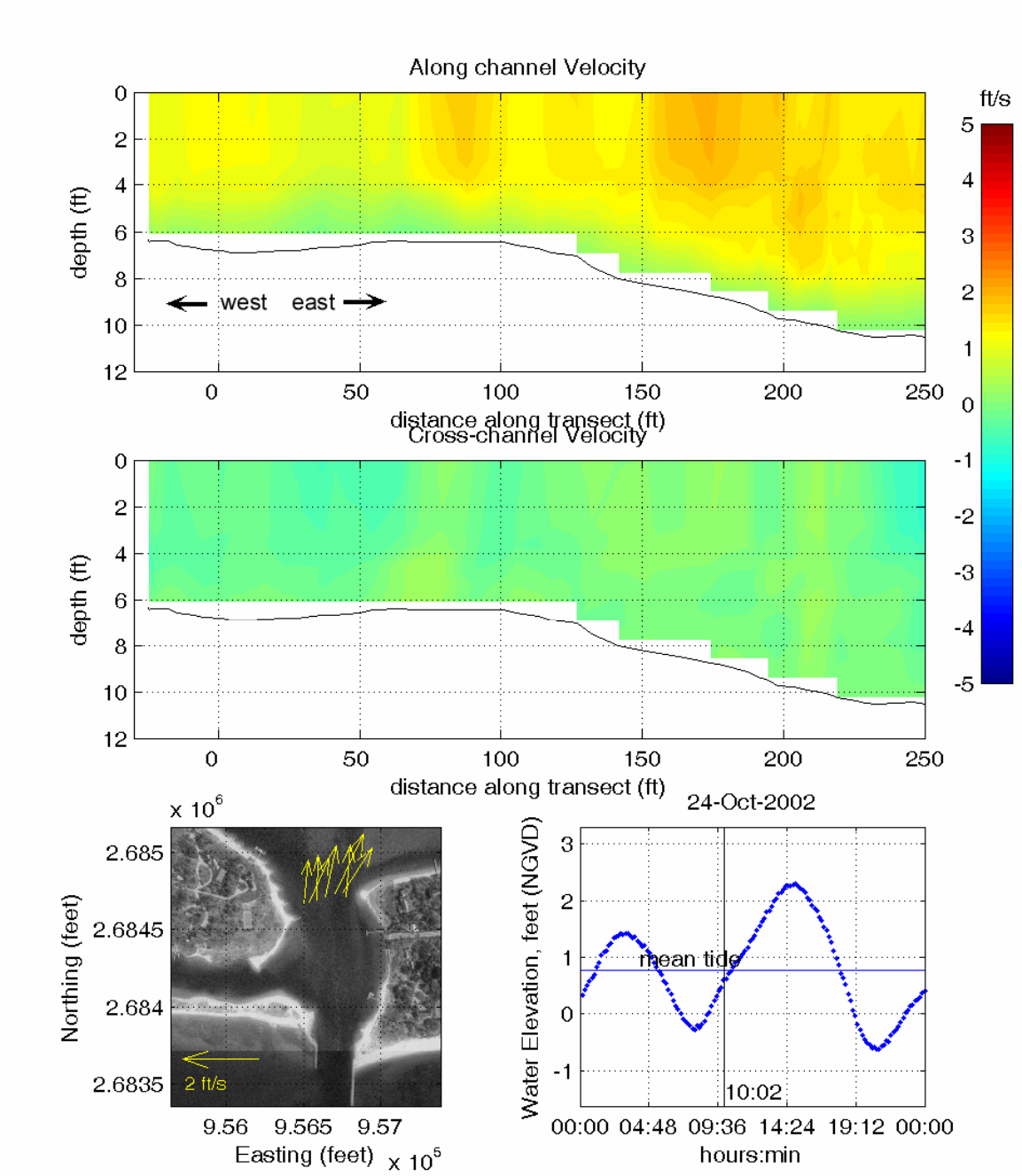

Figure V-16. Color contour plots of along-channel and cross-channel velocity components for transect line run east-to-west across the entrance to West Bay, measured at 10:02 on October 24, 2001 during the period of maximum flood tide currents. Positive along-channel currents (top panel) indicate the flow is moving into the estuary, while positive cross-channel velocities (middle panel) are oriented 90° clockwise of positive along-channel. Lower left plot shows scaled velocity vectors projected onto a 1994 aerial photo of the survey area. A tide plot for the survey day is also given.

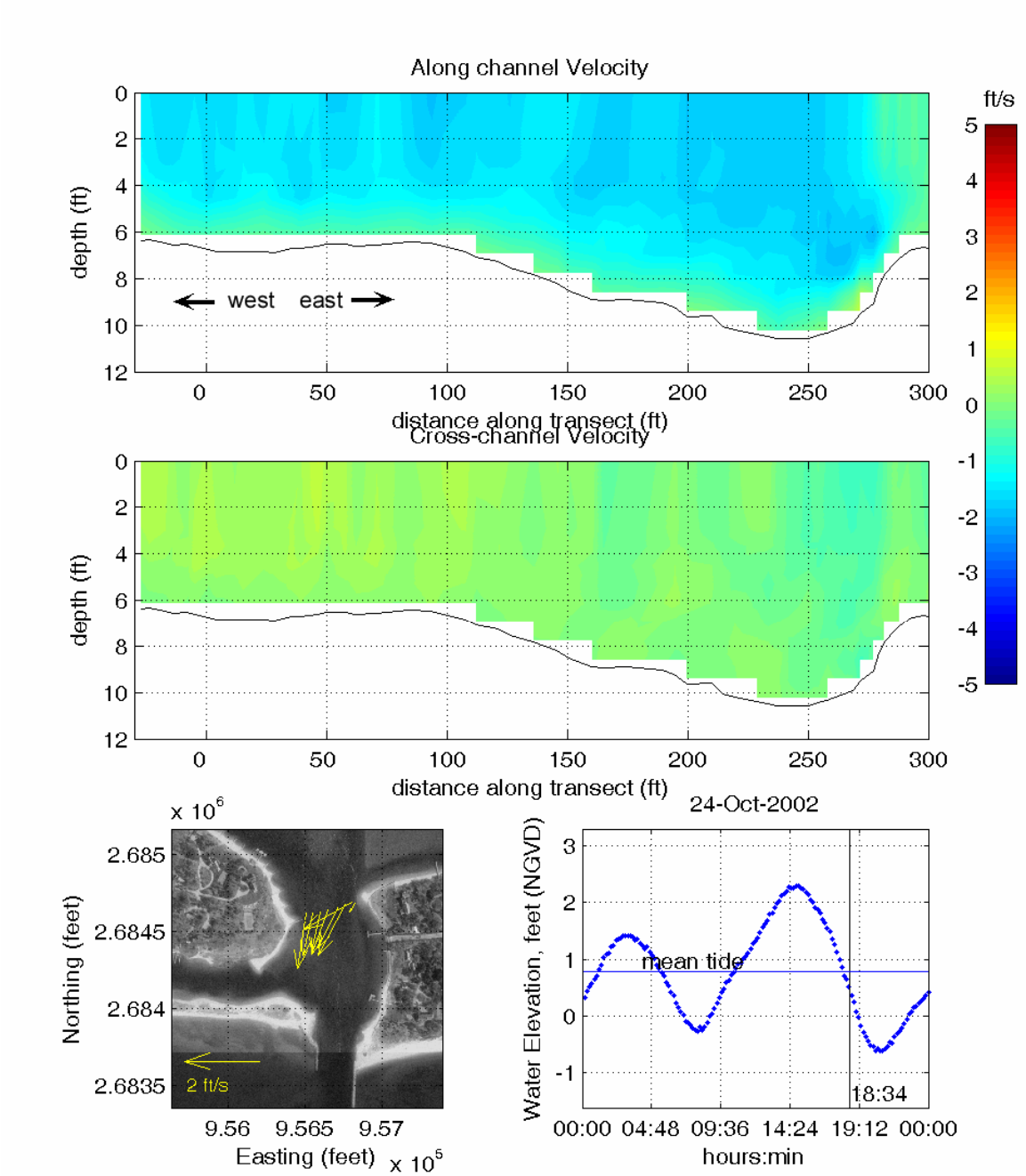

Figure V-17. Color contour plots of along-channel and cross-channel velocity components for transect line run east-to-west across the entrance to West Bay, measured at 18:34 on October 24, 2001 during the period of maximum ebb tide currents. Positive along-channel currents (top panel) indicate the flow is moving into the estuary, while positive cross-channel velocities (middle panel) are oriented 90° clockwise of positive along-channel. Lower left plot shows scaled velocity vectors projected onto a 1994 aerial photo of the survey area. A tide plot for the survey day is also given.

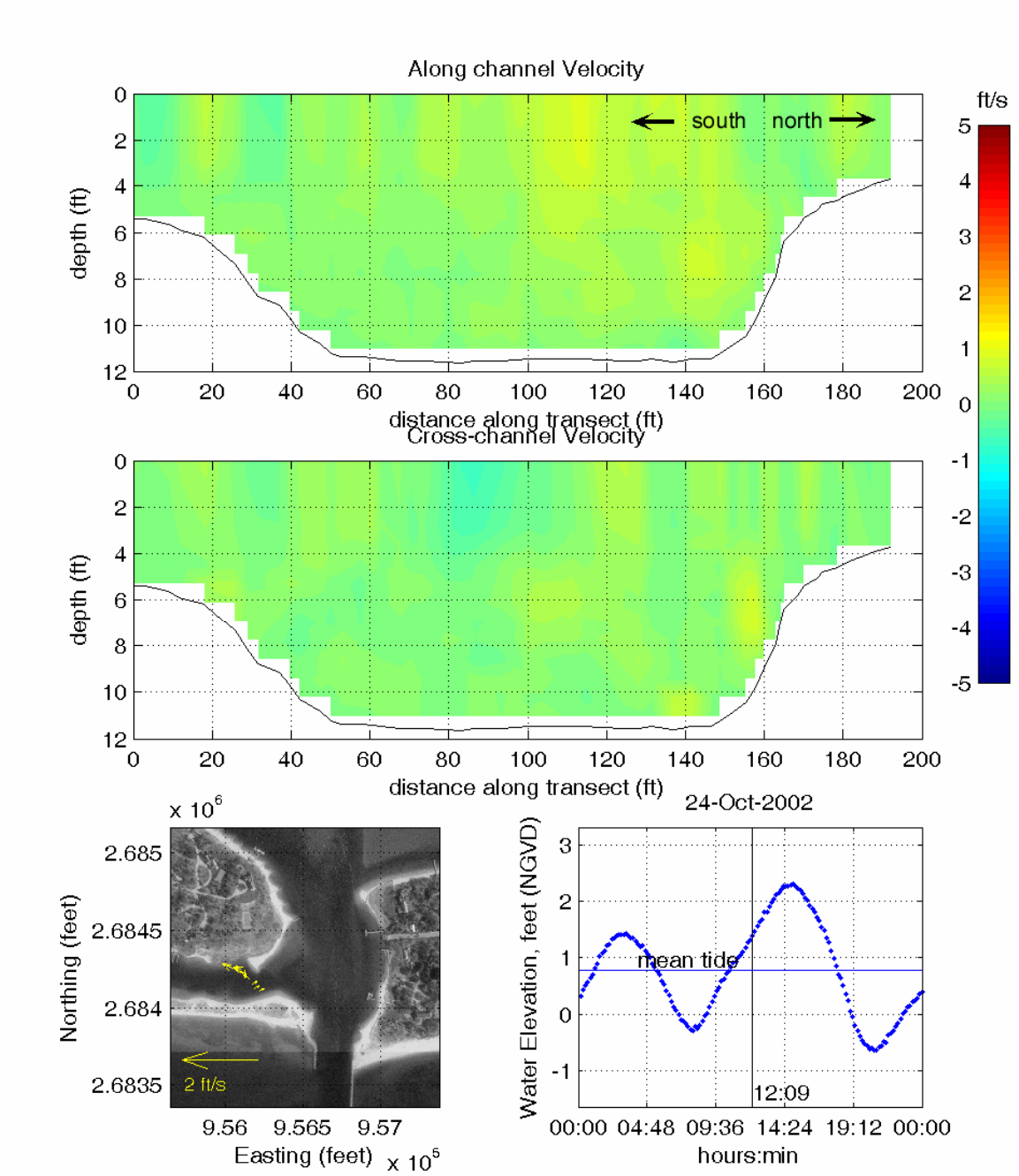

Figure V-18. Color contour plots of along-channel and cross-channel velocity components for transect line run north-to-south across the eastern end of the Seapuit River, measured at 12:09 on October 24, 2001 during the period of maximum flood tide currents. Positive along-channel currents (top panel) indicate the flow is moving into the estuary, while positive cross-channel velocities (middle panel) are oriented 90° clockwise of positive along-channel. Lower left plot shows scaled velocity vectors projected onto a 1994 aerial photo of the survey area. A tide plot for the survey day is also given.

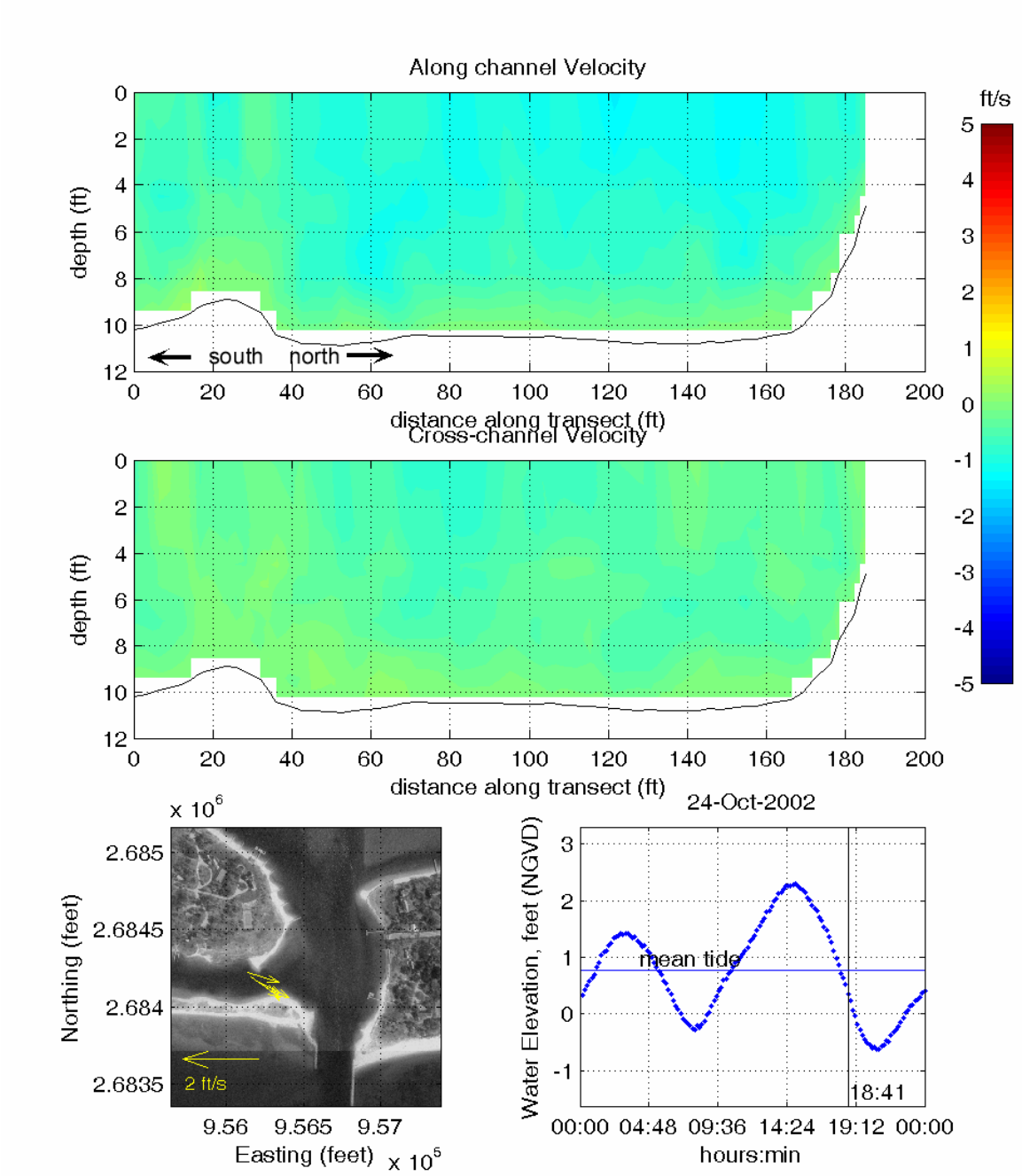

Figure V-19. Color contour plots of along-channel and cross-channel velocity components for transect line run east-to-west across the eastern end of the Seapuit River, measured at 18:41on October 24, 2001 during the period of maximum ebb tide currents. Positive along-channel currents (top panel) indicate the flow is moving into Cotuit Bay from the West Bay inlet, while positive cross-channel velocities (middle panel) are oriented 90° clockwise of positive along-channel. Lower left plot shows scaled velocity vectors projected onto a 1994 aerial photo of the survey area. A tide plot for the survey day is also given.

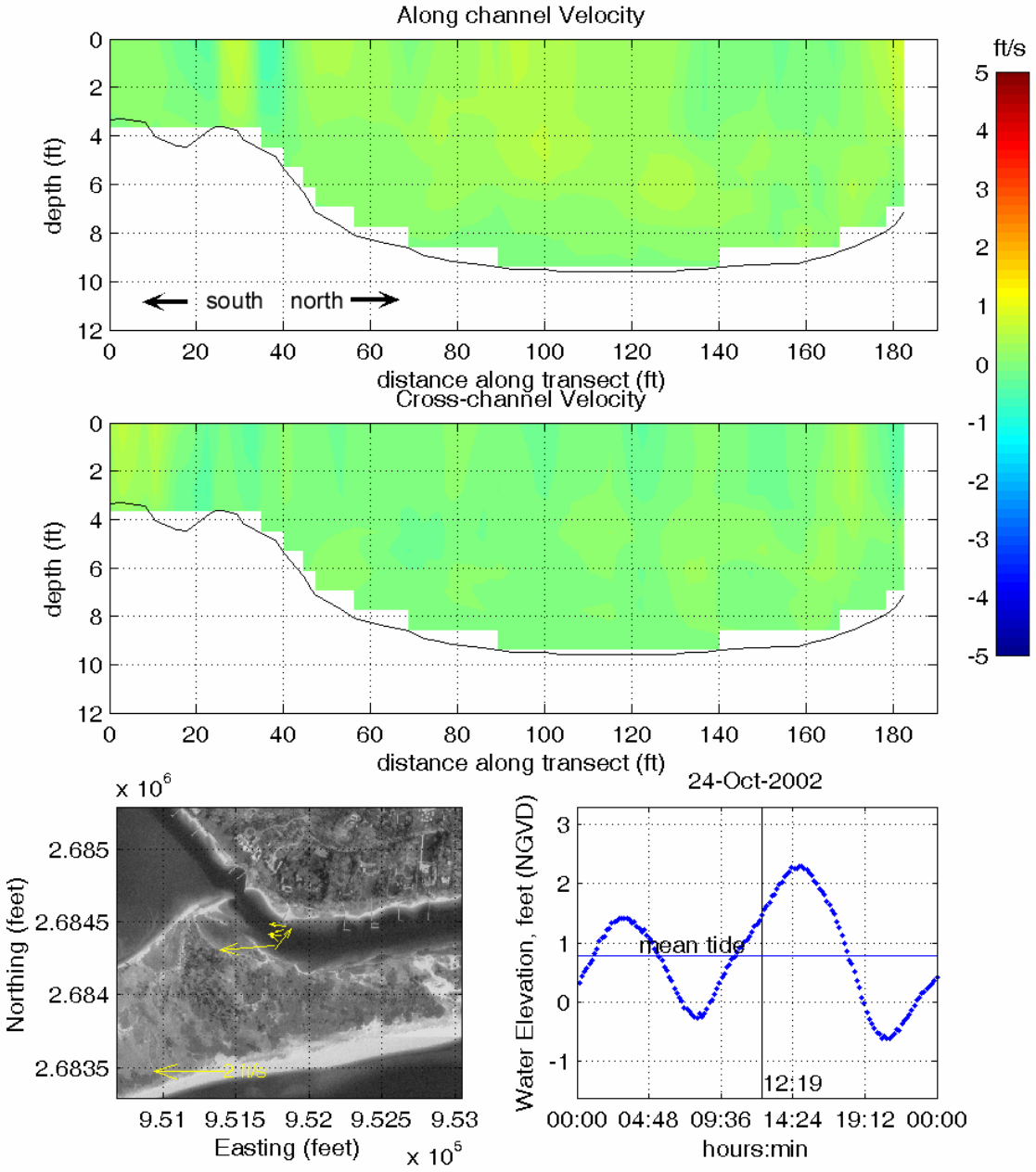

Figure V-20. Color contour plots of along-channel and cross-channel velocity components for transect line run north-to-south across the western end of the Seapuit River, measured at 12:19 on October 24, 2001 during the period of maximum flood tide currents. Positive along-channel currents (top panel) indicate the flow is moving into Cotuit Bay from the West Bay inlet, while positive cross-channel velocities (middle panel) are oriented 90° clockwise of positive along-channel. Lower left plot shows scaled velocity vectors projected onto a 1994 aerial photo of the survey area. A tide plot for the survey day is also given.

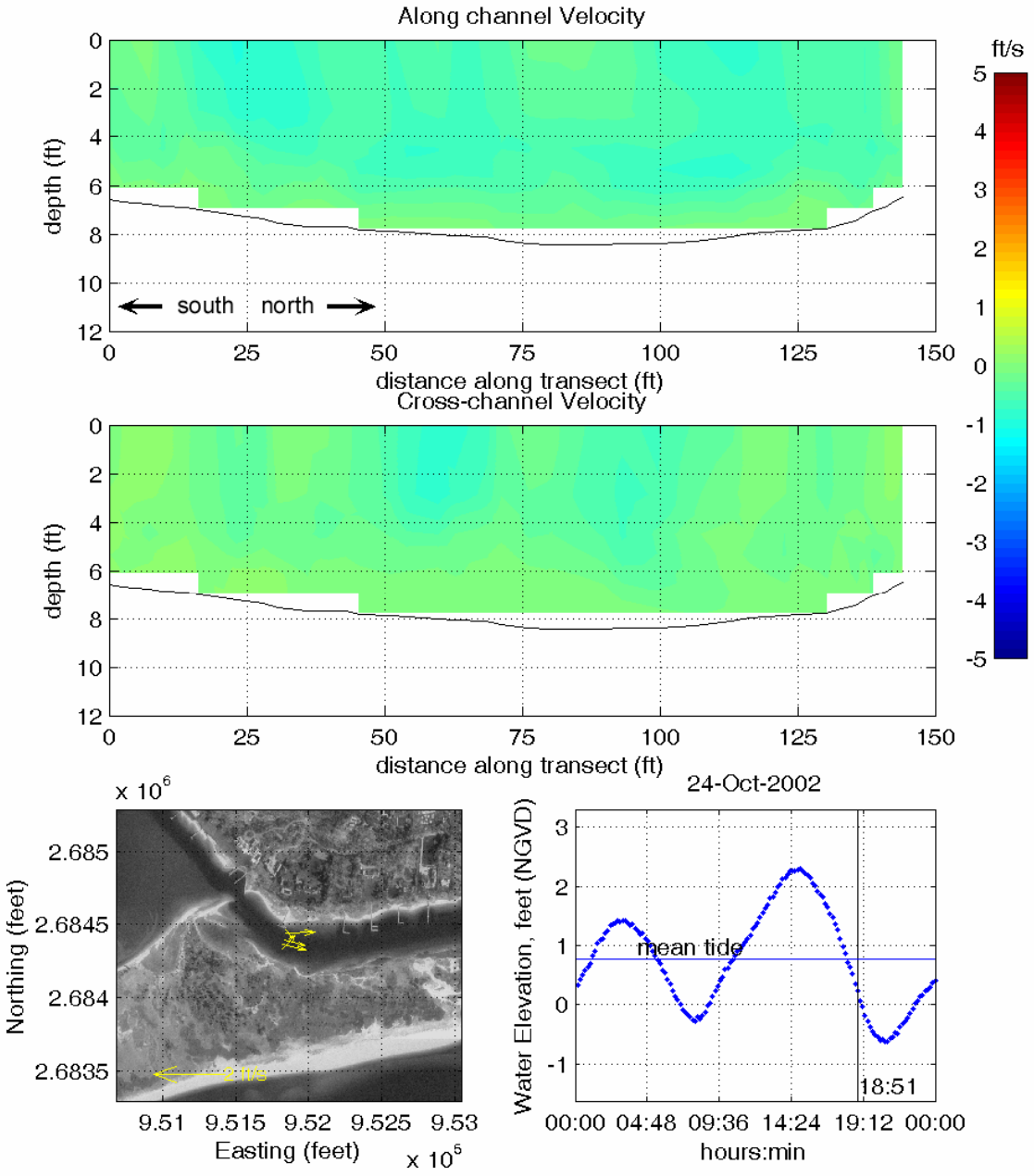

Figure V-21. Color contour plots of along-channel and cross-channel velocity components for transect line run north-to-south across the western end of the Seapuit River, measured at 18:51 on October 24, 2001 during the period of maximum ebb tide currents. Positive along-channel currents (top panel) indicate the flow is moving into Cotuit Bay from the West Bay inlet, while positive cross-channel velocities (middle panel) are oriented 90° clockwise of positive along-channel. Lower left plot shows scaled velocity vectors projected onto a 1994 aerial photo of the survey area. A tide plot for the survey day is also given.

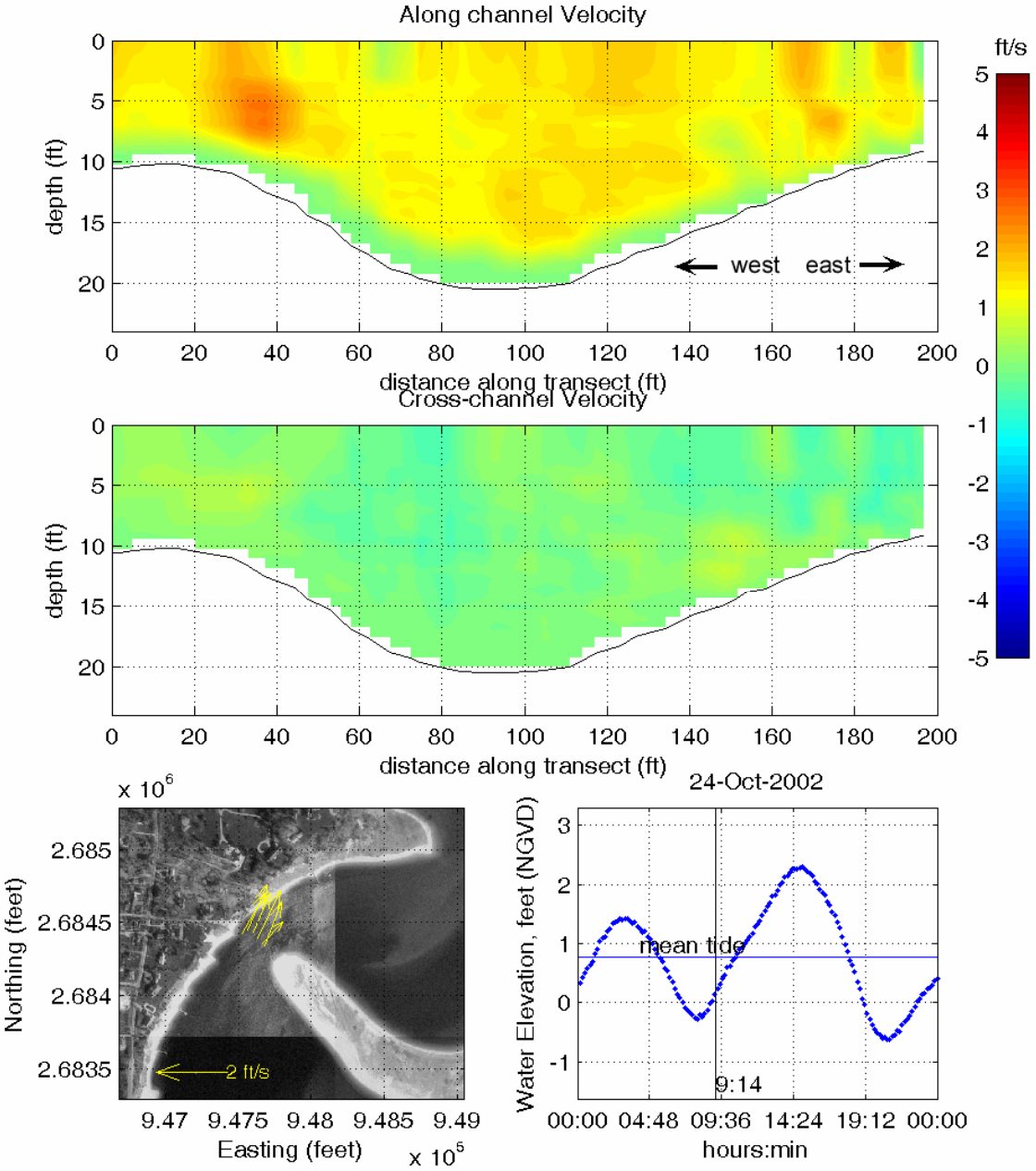

Figure V-22. Color contour plots of along-channel and cross-channel velocity components for transect line run west-to-east across Cotuit Bay Inlet, measured at 9:14 on October 24, 2001 during the period of maximum flood tide currents. Positive along-channel currents (top panel) indicate the flow is moving into the estuary, while positive cross-channel velocities (middle panel) are oriented 90° clockwise of positive along-channel. Lower left plot shows scaled velocity vectors projected onto a 1994 aerial photo of the survey area. A tide plot for the survey day is also given.

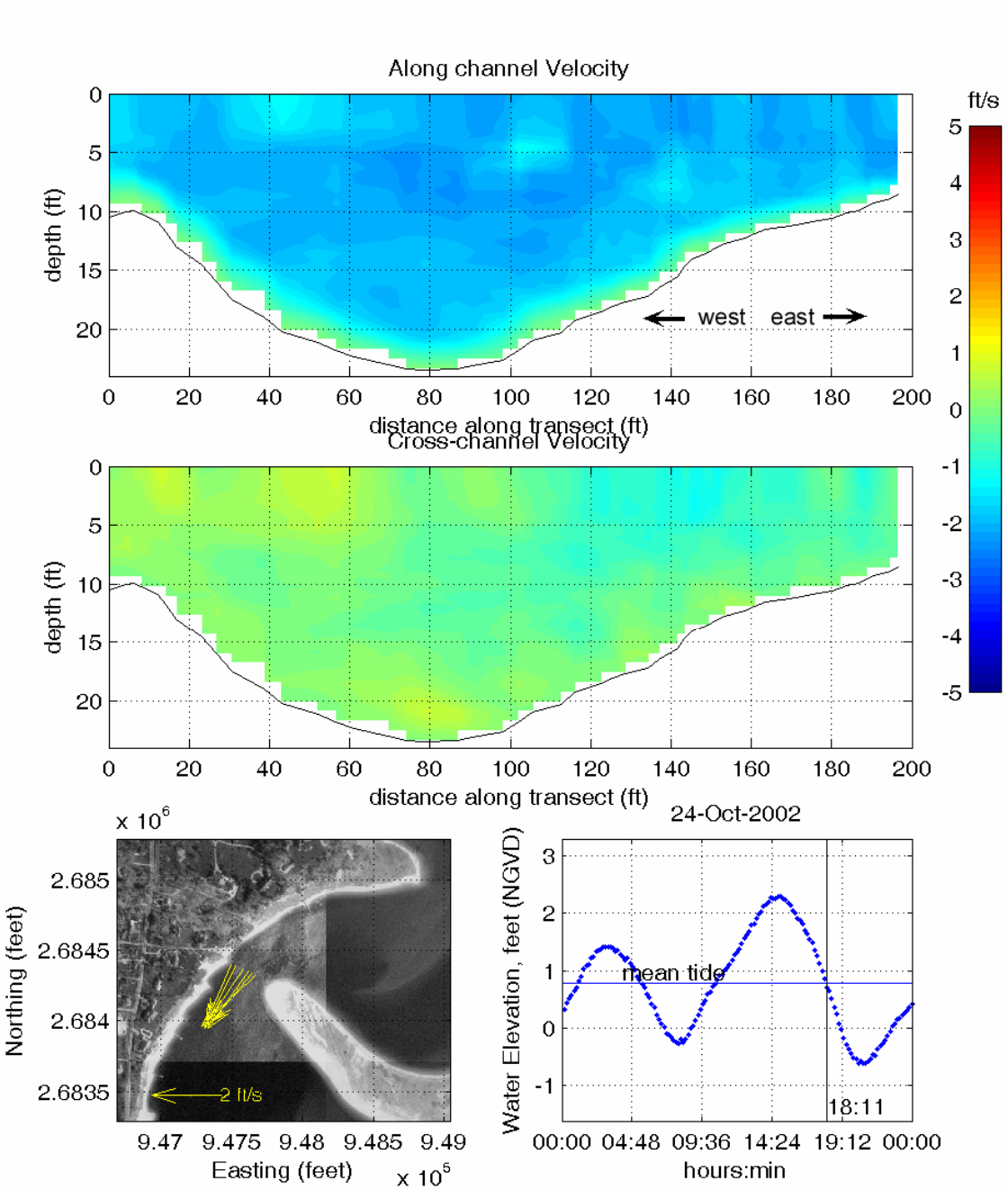

Figure V-23. Color contour plots of along-channel and cross-channel velocity components for transect line run west-to-east across Cotuit Bay Inlet, measured at 18:11 on October 24, 2001 during the period of maximum ebb tide currents. Positive along-channel currents (top panel) indicate the flow is moving into the estuary, while positive cross-channel velocities (middle panel) are oriented 90° clockwise of positive along-channel. Lower left plot shows scaled velocity vectors projected onto a 1994 aerial photo of the survey area. A tide plot for the survey day is also given.

V.4 HYDRODYNAMIC MODELING

For the modeling of the Three Bays system, Applied Coastal utilized a state-of-the-art computer model to evaluate tidal circulation and flushing in these systems. The particular model employed was the RMA-2 model developed by Resource Management Associates (King, 1990). It is a two-dimensional, depth-averaged finite element model, capable of simulating transient hydrodynamics. The model is widely accepted and tested for analyses of estuaries or rivers. Applied Coastal staff members have utilized RMA-2 for numerous flushing studies on Cape Cod, including West Falmouth Harbor, Popponesset Bay, Chatham embayments (Kelley, *et al*, 2001), Falmouth "finger" Ponds (Ramsey, *et al*, 2000), and Barnstable Harbor (Wood, *et al*, 1999).

V.4.1 Model Theory

In its original form, RMA-2 was developed by William Norton and Ian King under contract with the U.S. Army Corps of Engineers (Norton et al., 1973). Further development included the introduction of one-dimensional elements, state-of-the-art pre- and post-processing data programs, and the use of elements with curved borders. Recently, the graphic pre- and post-processing routines were updated by a Brigham Young University through a package called the Surfacewater Modeling System or SMS (BYU, 1998). Graphics generated in support of this report primarily were generated within the SMS modeling package.

RMA-2 is a finite element model designed for simulating one- and two-dimensional depth-averaged hydrodynamic systems. The dependent variables are velocity and water depth, and the equations solved are the depth-averaged Navier Stokes equations. Reynolds assumptions are incorporated as an eddy viscosity effect to represent turbulent energy losses. Other terms in the governing equations permit friction losses (approximated either by a Chezy or Manning formulation), Coriolis effects, and surface wind stresses. All the coefficients associated with these terms may vary from element to element. The model utilizes quadrilaterals and triangles to represent the prototype system. Element boundaries may either be curved or straight.

The time dependence of the governing equations is incorporated within the solution technique needed to solve the set of simultaneous equations. This technique is implicit; therefore, unconditionally stable. Once the equations are solved, corrections to the initial estimate of velocity and water elevation are employed, and the equations are re-solved until the convergence criteria is met.

V.4.2 Model Setup

There are three main steps required to implement RMA-2:

- Grid generation
- Boundary condition specification
- Calibration

The extent of each finite element grid was generated using 1994 digital aerial photographs from the MassGIS online orthophoto database. A time-varying water surface elevation boundary condition (measured tide) was specified at the entrances of the Three Bays system (i.e., Cotuit Bay Inlet and West Bay Inlet) based on the tide gauge data collected offshore Dead Neck, in Nantucket Sound. Once the grid and boundary conditions were set, the model was calibrated to ensure accurate predictions of tidal flushing. Various friction and eddy viscosity coefficients were adjusted, through several (10) model calibration simulations for each system,

to obtain agreement between measured and modeled tides. The calibrated model provides the requisite information for future detailed water quality modeling.

V.4.2.1 Grid generation

The grid generation process was aided by the use of the SMS package. 1994 digital aerial orthophotos and recent bathymetry survey data were imported to SMS, and a finite element grid was created to represent the estuary. The aerial photographs were used to determine the land boundary of the system. Bathymetry data were interpolated to the developed finite element mesh of the system. The completed grid consists of 5,190 nodes, which describe 1766 total 2-dimensional (depth averaged) quadratic elements, and covers 1337 acres. The maximum nodal depth is –22.9 ft (NGVD 29), in the throat of Cotuit Inlet. The completed grid mesh of the Three Bays system is shown in Figure V-24, and grid bathymetry was shown previously in Figure V-9.

The finite element grid for the system provided the detail necessary to evaluate accurately the variation in hydrodynamic properties throughout the Three Bays embayments. The SMS grid generation program was used to develop quadrilateral and triangular two-dimensional elements throughout the estuary. Grid resolution was governed by two factors: 1) expected flow patterns, and 2) the bathymetric variability of the system. Relatively fine grid resolution was employed where complex flow patterns were expected. For example, smaller node spacing in tidal creeks and channels was designed to provide a more detailed analysis in these regions of rapidly varying flow (e.g., the Cotuit Inlet, West Bay Inlet, and the Marstons Mills River). Widely spaced nodes were often employed in areas where flow patterns are not likely to change dramatically, such as in the main bodies of Cotuit Bay, West Bay, North Bay, and Prince's Cove. Appropriate implementation of wider node spacing and larger elements reduced computer run time with no sacrifice of accuracy.

V.4.2.2 Boundary condition specification

Two types of boundary conditions were employed for the RMA-2 model of the Three Bays system: 1) "slip" boundaries, and 2) tidal elevation boundaries. All of the elements with land borders have "slip" boundary conditions, where the direction of flow was constrained shore-parallel. The model generated all internal boundary conditions from the governing conservation equations. Tidal boundary conditions were specified at both inlets from Nantucket Sound, Cotuit Bay Inlet and West Bay Inlet. TDR measurements from a gauge deployed offshore Dead Neck provided the required data.

The rise and fall of the tide in Nantucket Sound is the primary driving force for estuarine circulation in this system. Dynamic (time-varying) model simulations specified a new water surface elevation at Cotuit Inlet and West Bay Inlet every model time step of 10 minutes, which corresponds to the time step of the TDR data measurements. A time lag of 3 minutes was added to the tidal boundary condition at Cotuit inlet (lagging relative to West Bay Inlet) to account for the propagation of the tide from east to west. Over the 1.7-mile distance between the two inlets, the slight difference in tidal phase subtly affects the flow dynamics within the Three Bays system. Results from the RMA-2 model of the system show that the phase difference drives the flow through the Seapuit River. The 3 minute lag was determined based on the typical difference in time of high and low tides between Hyannisport and Cotuit, as publish in tide tables by NOAA. By this method, the tide propagates an average 2800 ft/min. Alternately, a similar result can be computed using the shallow wave equation $C = \sqrt{gh}$, where C is the speed of the tidal wave computed from the gravitational constant g, and the typical

water depth *h*. This method results in a phase delay of 5 minutes. Model results discussed later in this section show that the 3-minute delay induces the correct magnitude and flow direction in the Seapuit River.

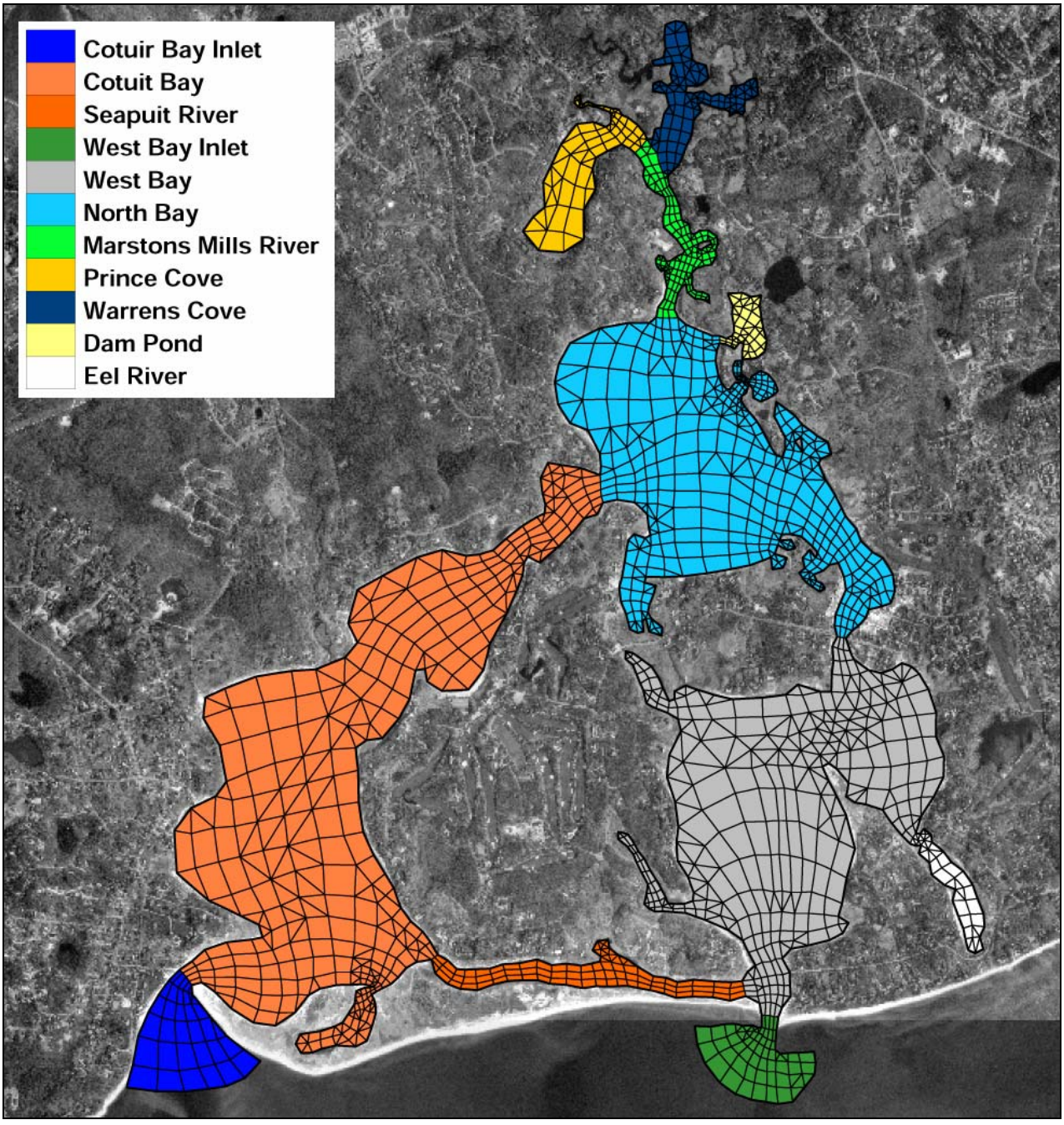

Figure V-24. Plot of hydrodynamic model grid mesh for the Three Bays system of Barnstable, MA. Color patterns designate the different model material types used to vary model calibration parameters and compute flushing rates.

V.4.2.3 Calibration

After developing the finite element grid, and specifying boundary conditions, the model for the Three Bays system was calibrated. The calibration procedure ensures that the model predicts accurately what was observed in nature during the field measurement program. Numerous model simulations are required (typically 20+) for an estuary model, specifying a range of friction and eddy viscosity coefficients, to calibrate the model.

Calibration of the hydrodynamic model required a close match between the modeled and measured tides in each of the sub-embayments where tides were measured (i.e., from the TDR deployments). Initially, the model was calibrated to obtain visual agreement between modeled and measured tides. Once visual agreement was achieved, a five lunar-day period (10 tide cycles) was modeled to calibrate the model based on dominant tidal constituents discussed in Section 3.2. The five-day period was extracted from a longer simulation to avoid effects of model spin-up, and to focus on average tidal conditions. Modeled tides for the calibration time period were evaluated for time (phase) lag and height damping of dominant tidal constituents.

The calibration was performed for a five-day period beginning October 8, 2002 1430 EST. This representative time period included the spring tide range of conditions, where the tide range and tidal currents are greatest, and model numerical stability is often most sensitive. To provide average tidal forcing conditions for model verification and the flushing analysis, a separate time period was chosen that spanned the transition between spring and neap tide ranges (bi-weekly maximum and minimum tidal ranges, respectively). For model verification and the flushing analysis, the 7 lunar-day period (14 tide cycles, or 7.25 solar days) beginning October 11, 2002 0000 EST was used.

The calibrated model was used to analyze system flow patterns and compute residence times. The ability to model a range of flow conditions is a primary advantage of a numerical tidal flushing model. For instance, average residence times were computed using the entire seven-day simulation. Other methods, such as dye and salinity studies, evaluate tidal flushing over relatively short time periods (less than one day). These short-term measurement techniques may not be representative of average conditions due to the influence of unique, short-lived atmospheric events.

V.4.2.3.1 Friction coefficients

Friction inhibits flow along the bottom of estuary channels or other flow regions where velocities are relatively high. Friction is a measure of the channel roughness, and can cause both significant amplitude damping and phase delay of the tidal signal. Friction is approximated in RMA-2 as a Manning coefficient, and is applied to grid areas by user specified material types. Initially, Manning's friction coefficient values of 0.03 were specified for all element material types. This values corresponds to typical Manning's coefficients determined experimentally in smooth earth-lined channels with no weeds (low friction) (Henderson, 1966).

During calibration, friction coefficients were incrementally changed throughout the model domain. Final model calibration runs incorporated various specific values for Manning's friction coefficients, depending upon flow damping characteristics of separate regions within the estuary system. Manning's values for different bottom types were initially selected based ranges provided by the Civil Engineering Reference Manual (Lindeburg, 1992), and values were incrementally changed when necessary to obtain a close match between measured and modeled tides. Final calibrated friction coefficients are summarized in the Table V-5.

Table V-5. Manning's Roughness coefficients used in simulations of modeled embayments. These embayment delineations correspond to the material type areas shown in Figure V-24.

System Embayment	Bottom Friction
Cotuit Bay Inlet	0.030
Cotuit Bay	0.030
Seapuit River	0.025
West Bay Inlet	0.030
West Bay	0.030
North Bay	0.030
Marstons Mills River	0.035
Prince's Cove	0.035
Warren's Cove	0.035
Dam Pond	0.030
Eel River	0.030

V.4.2.3.2 Turbulent exchange coefficients

Turbulent exchange coefficients approximate energy losses due to internal friction between fluid particles. The significance of turbulent energy losses increases where flow is swifter, such as inlets and bridge constrictions. According to King (1990), these values are proportional to element dimensions (numerical effects) and flow velocities (physics). Typically, model turbulence coefficients were set between 80 and 200 lb-sec/ft^2. In most cases, the Three Bays system was relatively insensitive to turbulent exchange coefficients. The exception was at the inlets, where higher exchange coefficient values (200 lb-sec/ft^2) were used to ensure numerical stability in these areas characterized by strong turbulent flows and large velocity magnitudes.

V.4.2.3.3 Wetting and Drying

Modeled hydrodynamics were complicated by wetting/drying cycles in shallow flats included in the model of the Three Bays system. A method was employed to simulate the periodic inundation and drying of tidal flats in the system. Nodal wetting and drying is a feature of RMA-2 that allows grid elements to be removed and re-inserted during the course of the model run. The wetting and drying feature has two keys benefits for the simulation, 1) it enhances the stability of the model by eliminating nodes that have bottom elevations that are higher than the water surface elevation at that time, and 2) it reduces total model run time because node elimination can reduce the size of the computational grid significantly during periods of a model run. Wetting and drying is employed for estuarine systems with relatively shallow borders and/or tidal flats.

V.4.2.3.4 Comparison of modeled tides and measured tide data

A best-fit of model predictions for the TDR deployment was achieved using the aforementioned values for friction and turbulent exchange. Figures V-25 through and V-31 illustrate the five-day calibration simulation along with a 50-hour sub-section. Modeled (solid line) and measured (dotted line) tides are illustrated at each model location with a corresponding TDR.

Although visual calibration achieved reasonable modeled tidal hydrodynamics, further tidal constituent calibration was required to quantify the accuracy of the models. Calibration of M_2

(principle lunar semidiurnal constituent) was the highest priority since M_2 accounted for a majority of the forcing tide energy in the modeled systems. Due to the duration of the model runs, four dominant tidal constituents were selected for constituent comparison: K_1, M_2, M_4, and M_6. Measured tidal constituent heights (H) and time lags (ϕ_{lag}) shown in Table V-6 for the calibration period differ from those in Table V-2 because constituents were computed for only the five-day section of the 38-days represented in Table W. Table V-6 compares tidal constituent amplitude (height) and relative phase (time) for modeled and measured tides at the TDR locations. The constituent phase shows the relative timing of each separate constituent at a particular location, and also the change (or phase lag) in timing of a single constituent at different locations in an estuary.

The constituent calibration resulted in excellent agreement between modeled and measured tides. The largest errors associated with tidal constituent amplitude were on the order of 0.01 ft, which is better than the order of accuracy of the tide gauges (±0.12 ft). Time lag errors were typically less than the time increment resolved by the model (1/6 hours or 10 minutes), indicating good agreement between the model and data.

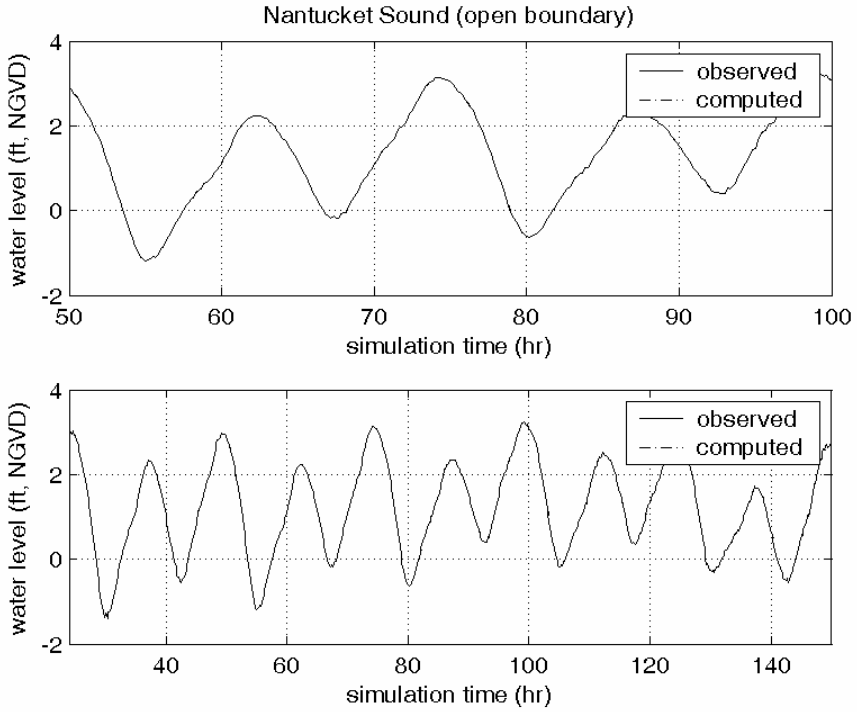

Figure V-25. Comparison of model output and measured tides for the TDR location offshore Dead Neck, in Nantucket Sound. The top plot is a 50-hour sub-section of the total modeled time period, shown in the bottom plot.

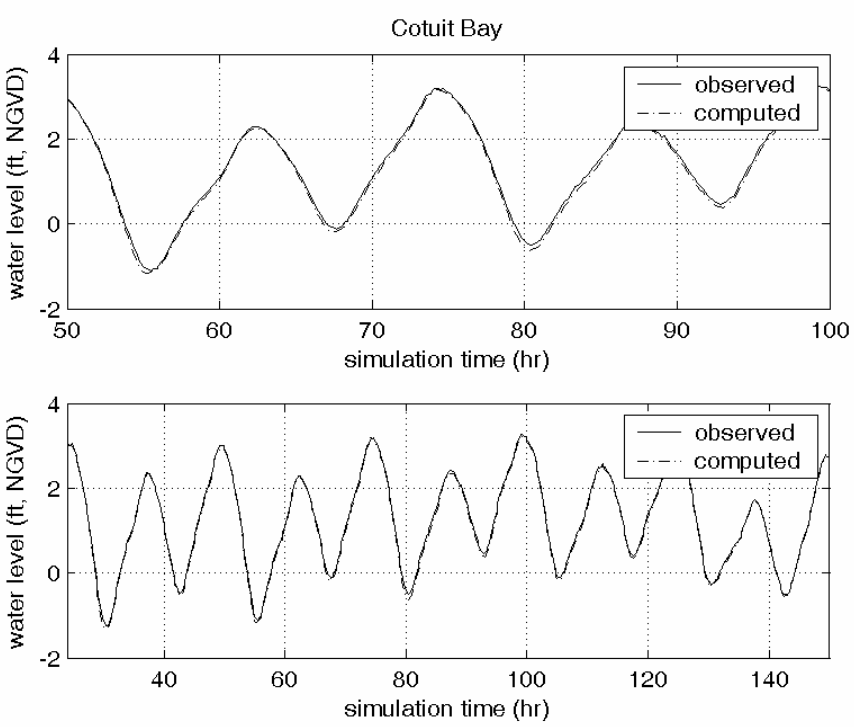

Figure V-26. Comparison of model output and measured tides for the TDR location in lower Cotuit Bay. The top plot is a 50-hour sub-section of the total modeled time period, shown in the bottom plot.

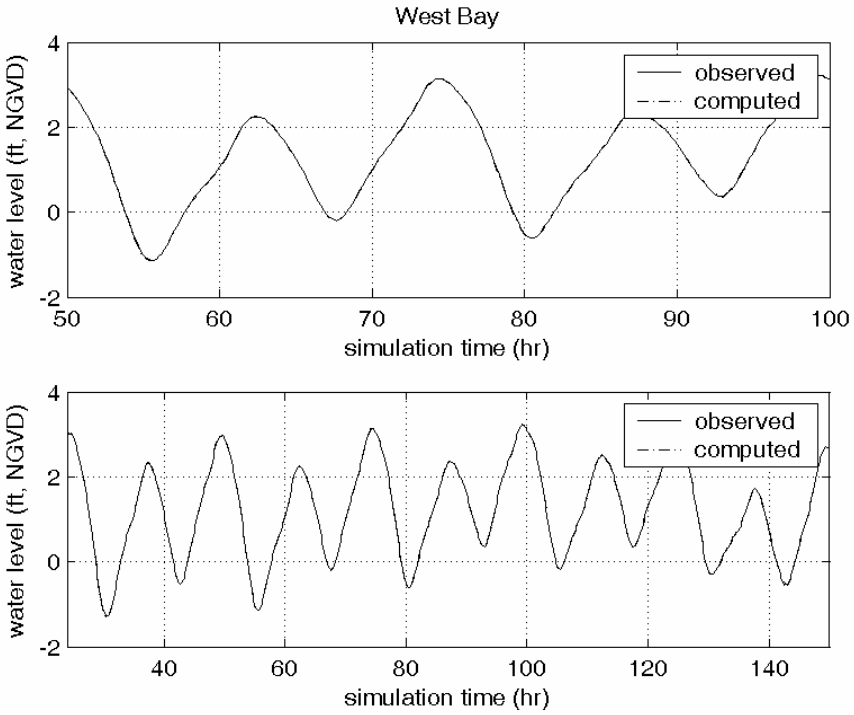

Figure V-27. Comparison of model output and measured tides for the TDR location in West Bay. The top plot is a 50-hour sub-section of the total modeled time period, shown in the bottom plot.

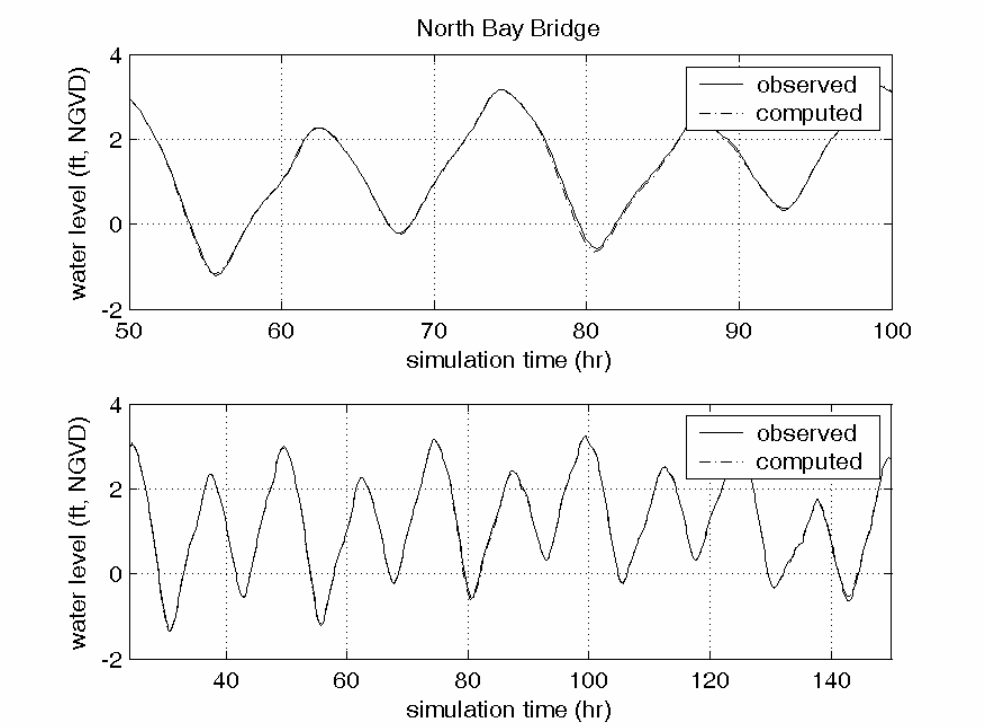

Figure V-28. Comparison of model output and measured tides for the TDR location at Oyster Harbors Marina, near the Little Island draw bridge. The top plot is a 50-hour sub-section of the total modeled time period, shown in the bottom plot.

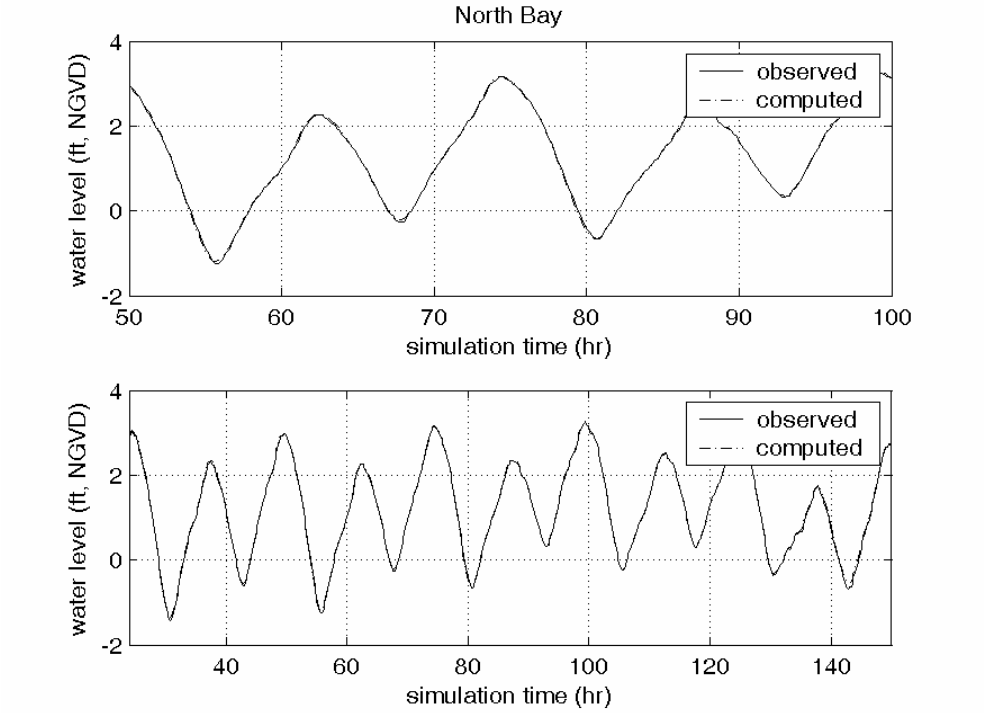

Figure V-29. Comparison of model output and measured tides for the TDR location in North Bay, off Point Isabelle. The top plot is a 50-hour sub-section of the total modeled time period, shown in the bottom plot.

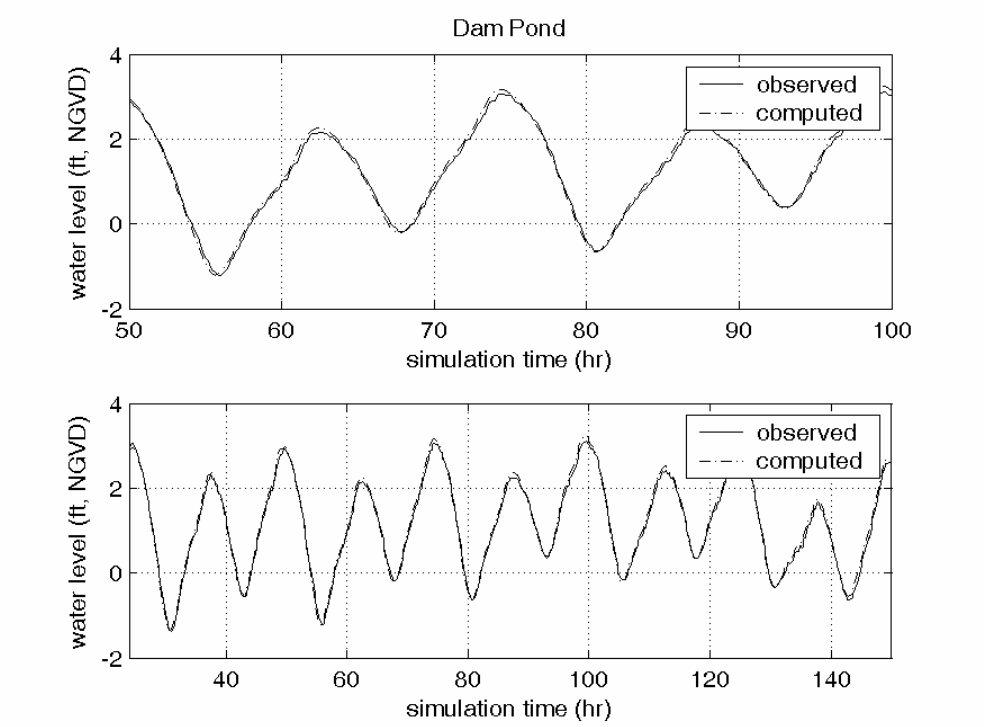

Figure V-30. Comparison of model output and measured tides for the TDR location in Dam Pond. The top plot is a 50-hour sub-section of the total modeled time period, shown in the bottom plot.

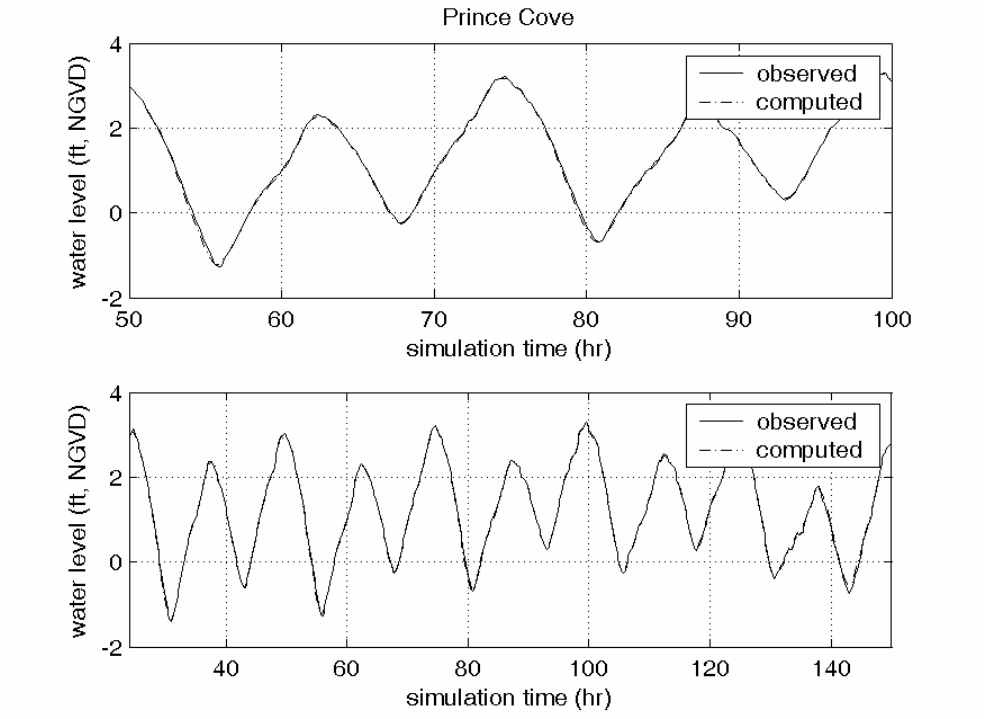

Figure V-31. Comparison of model output and measured tides for the TDR location in Prince's Cove. The top plot is a 50-hour sub-section of the total modeled time period, shown in the bottom plot.

V.4.2.4 Model Verification

The calibration procedure used in the development of the Three Bays finite-element model required a match between measured and modeled tides. An additional model verification run was performed to verify the model performance during time periods different from the calibration time period. In this fashion, the calibrated model is tested to ensure its accuracy when run for any time period outside the calibration period. The results of the model verification runs are shown in Table V-7. The analysis of the verification model runs in this table shows that the model performs with a similar excellent degree of accuracy to the calibration runs.

Table V-6. Tidal constituents for measured water level data and calibrated model output, with model error amplitudes, for the Three-Bays system, during modeled calibration time period.

Model calibration run						
Location	Constituent Amplitude (ft)				Phase (deg)	
	M_2	M_4	M_6	K_1	ϕM_2	ϕM_4
Nantucket Sound*	1.39	0.20	0.09	0.41	26.0	152.8
Cotuit Bay	1.39	0.20	0.09	0.42	30.2	162.2
West Bay	1.39	0.18	0.10	0.42	31.2	165.7
North Bay Bridge	1.39	0.18	0.11	0.42	33.0	172.2
North Bay	1.40	0.17	0.11	0.42	33.4	174.0
Dam Pond	1.40	0.17	0.11	0.42	33.8	175.0
Prince's Cove	1.40	0.17	0.12	0.42	35.5	180.5
Measured tide during calibration period						
Location	Constituent Amplitude (ft)				Phase (deg)	
	M_2	M_4	M_6	K_1	ϕM_2	ϕM_4
Nantucket Sound*	1.39	0.20	0.09	0.41	26.0	152.7
Cotuit Bay	1.37	0.19	0.10	0.41	30.1	164.3
West Bay	1.38	0.18	0.10	0.41	31.0	167.4
North Bay Bridge	1.39	0.17	0.11	0.40	33.5	176.6
North Bay	1.38	0.18	0.10	0.41	33.8	178.8
Dam Pond	1.35	0.17	0.12	0.41	37.5	185.5
Prince's Cove	1.39	0.16	0.13	0.41	35.9	185.4
Error						
Location	Error Amplitude (ft)				Phase error (min)	
	M_2	M_4	M_6	K_1	ϕM_2	ϕM_4
Nantucket Sound*	0.00	0.00	0.00	0.00	0	0
Cotuit Bay	0.02	0.01	-0.01	0.01	0	0
West Bay	0.01	0.00	0.00	0.01	0	2
North Bay Bridge	0.00	0.01	0.00	0.02	1	5
North Bay	0.02	-0.01	0.01	0.01	1	5
Dam Pond	0.05	0.00	-0.01	0.01	8	11
Prince's Cove	0.01	0.01	-0.01	0.01	1	5

*model open boundary

Table V-7. Tidal constituents for measured water level data and calibrated model output, with model error amplitudes, for the Three-Bays system, during modeled verification time period.

Model verification run						
Location	Constituent Amplitude (ft)				Phase (deg)	
	M_2	M_4	M_6	K_1	ϕM_2	ϕM_4
Nantucket Sound*	1.13	0.17	0.06	0.40	175.8	93.2
Cotuit Bay	1.13	0.16	0.07	0.40	179.7	102.2
West Bay	1.13	0.16	0.07	0.40	180.5	105.0
North Bay Bridge	1.13	0.15	0.07	0.40	182.1	110.0
North Bay	1.14	0.16	0.08	0.40	182.4	111.3
Dam Pond	1.14	0.15	0.08	0.40	182.7	112.1
Prince's Cove	1.14	0.15	0.08	0.40	184.4	116.7
Measured tide during verification period						
Location	Constituent Amplitude (ft)				Phase (deg)	
	M_2	M_4	M_6	K_1	ϕM_2	ϕM_4
Nantucket Sound*	1.13	0.17	0.07	0.40	176.1	92.1
Cotuit Bay	1.12	0.16	0.07	0.40	179.5	102.2
West Bay	1.13	0.16	0.08	0.39	184.5	119.8
North Bay Bridge	1.13	0.16	0.08	0.39	182.3	112.2
North Bay	1.13	0.16	0.07	0.39	180.4	105.7
Dam Pond	1.09	0.16	0.09	0.40	187.8	124.9
Prince's Cove	1.13	0.16	0.09	0.40	184.5	119.8
Error						
Location	Error Amplitude (ft)				Phase error (min)	
	M_2	M_4	M_6	K_1	ϕM_2	ϕM_4
Nantucket Sound*	0.00	0.00	-0.01	0.00	1	-1
Cotuit Bay	0.01	0.00	0.00	0.00	-1	0
West Bay	0.00	0.00	-0.01	0.01	0	1
North Bay Bridge	0.00	-0.01	-0.01	0.01	1	2
North Bay	0.01	0.00	0.01	0.01	1	3
Dam Pond	0.05	-0.01	-0.01	0.00	10	13
Prince's Cove	0.01	-0.01	-0.01	0.00	0	3

*model open boundary

V.4.2.5 ADCP verification of the Three Bays system

An additional model verification check was possible by using collected ADCP velocity data to verify the performance of the Three Bays system model. Computed flow rates from the model were compared to flow rates determined using the measured velocity data. The ADCP data survey efforts are described in Section 2. For the model ADCP verification, the Three Bays model was run for the period covered during the ADCP survey on October 24, 2002. Model flow rates were computed in RMA-2 at continuity lines (channel cross-sections) that correspond to the actual ADCP transects followed in each survey (i.e., across each inlet, at the entrance to West Bay, and at the east and west ends of the Seapuit River).

Comparisons of the measured and modeled volume flow rates in the Three Bays system are shown in Figures V-32 through V-36. For each figure, the top plot shows the flow

comparison, and the lower plot shows the time series of tide elevation for the same period. Each ADCP point (blue triangles shown on the plots) is a summation of flow measured along the ADCP transect. The 'bumps' and 'skips' of the flow rate curve (more evident in the model output) can be attributed to the effects of winds (i.e., atmospheric effects) on the water surface and friction across the seabed periodically retarding or accelerating the flow through the inlets, and inside the system channels. If water surface elevations changed smoothly as a sinusoid, the volume flow rate would also appear as a smooth curve. However, since the rate at which water surface elevations change does not vary smoothly, the flow rate curve is expected to show short-period fluctuations.

Data comparisons at all five ADCP transect show exceptionally good agreement with the model predictions. The calibrated model accurately describes the discharge magnitude at each line, even in the Seapuit River where flow rates are an order of magnitude less than at each inlet. For all transects the R^2 correlation coefficients between data and model results are between 0.99 and 0.83. The lowest correlation is at the West Seapuit transect (R^2 value of 0.83) which is still good considering the low volume flow rates, which are more difficult to measure at this transect. Correlation statistics between the modeled and measured flows for each ADCP transect are presented in Table V-8.

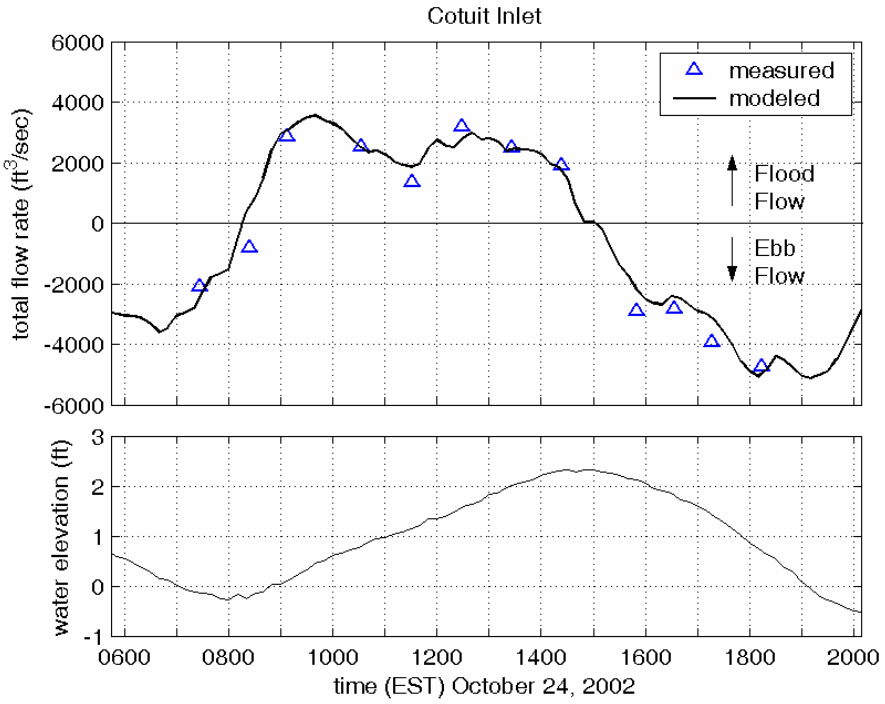

Figure V-32. Comparison of measured volume flow rates versus modeled flow rates (top plot) through the Cotuit Bay Inlet over a tidal cycle on October 24, 2001. Flood flows into the inlet are positive (+), and ebb flows out of the inlet are negative (-). The bottom plot shows the tide elevation offshore Dead Neck. (R^2 =0.96).

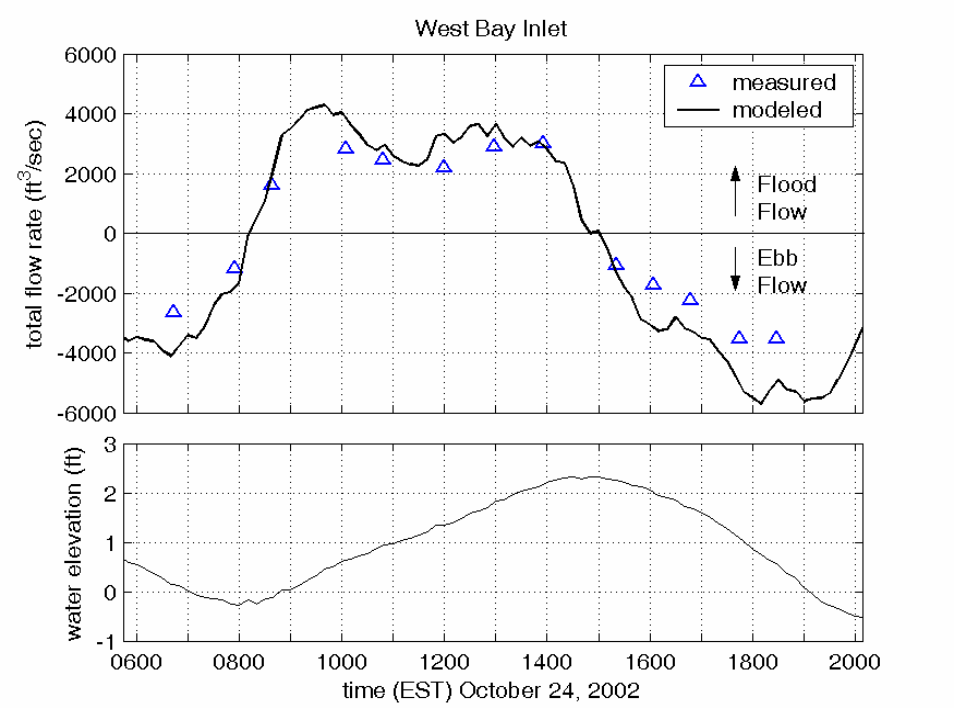

Figure V-33. Comparison of measured volume flow rates versus modeled flow rates (top plot) through West Bay Inlet over a tidal cycle on October 24, 2001. Flood flows into the inlet are positive (+), and ebb flows out of the inlet are negative (-). The bottom plot shows the tide elevation offshore Dead Neck. (R^2=0.84).

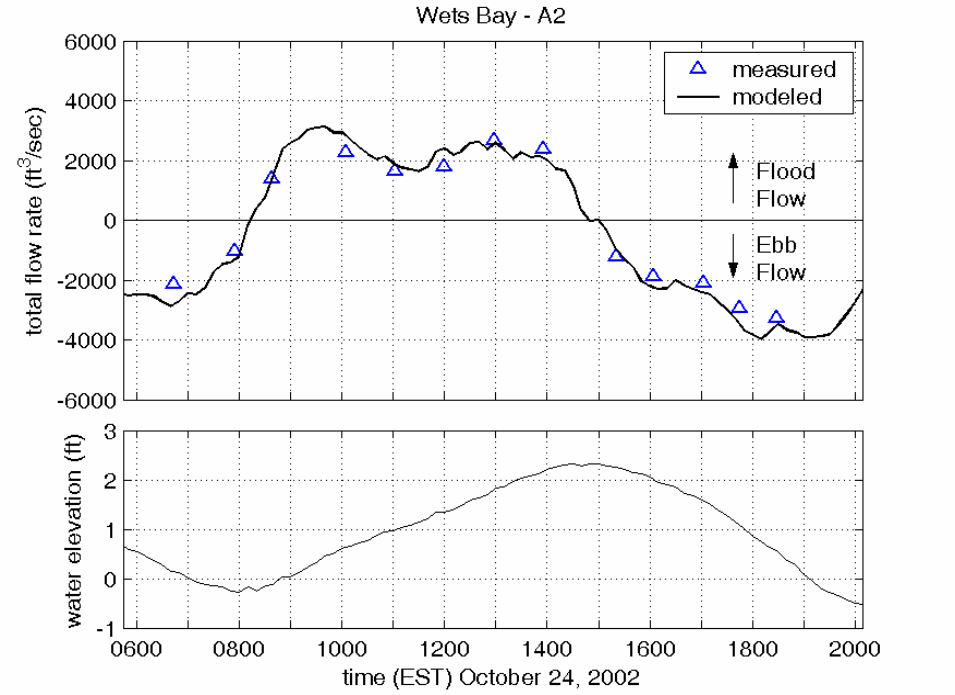

Figure V-34. Comparison of measured volume flow rates versus modeled flow rates (top plot) through the entrance to West Bay, at transect A2, over a tidal cycle on October 24, 2001. Flood flows into the bay are positive (+), and ebb flows out of the bay are negative (-). The bottom plot shows the tide elevation offshore Dead Neck. (R^2=0.97).

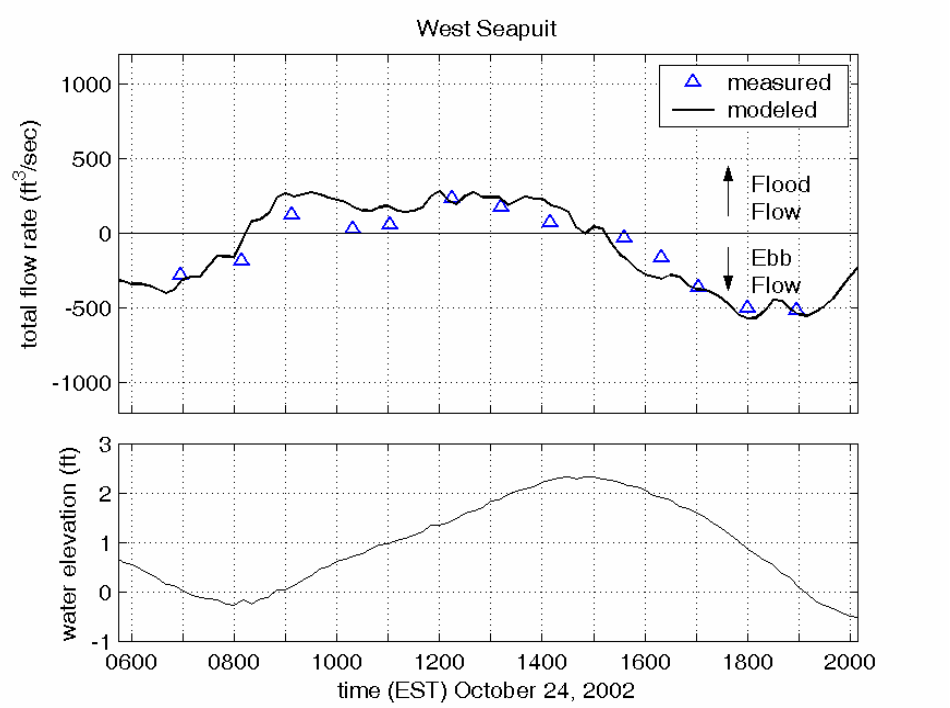

Figure V-35. Comparison of measured volume flow rates versus modeled flow rates (top plot) through the west entrance to the Seapuit River over a tidal cycle on October 24, 2001. Flood flows are positive (+), and ebb flows are negative (-). The bottom plot shows the tide elevation offshore Dead Neck. (R^2=0.83).

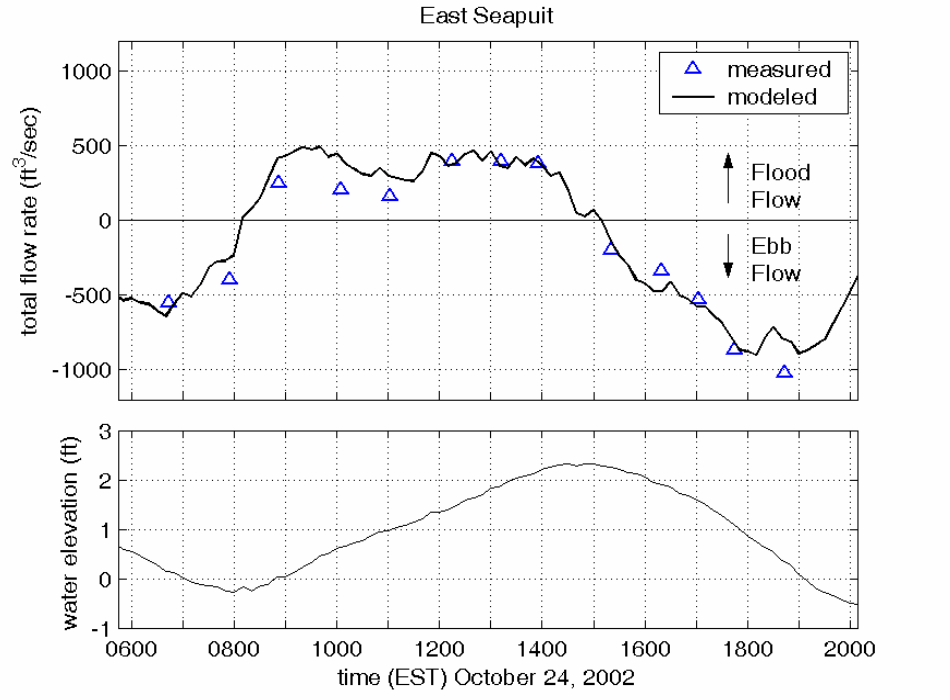

Figure V-36. Comparison of measured volume flow rates versus modeled flow rates (top plot) through the east entrance to the Seapuit River over a tidal cycle on October 24, 2001. Flood flows are positive (+), and ebb flows are negative (-). The bottom plot shows the tide elevation offshore Dead Neck. (R^2=0.94).

Table V-8. Correlation statistics between modeled and measured total flow rates at the five ADCP transects				
Transect	R^2 correlation	RMS error (ft^3/sec)	Max Error (ft^3/sec)	Min Error (ft^3/sec)
Cotuit Bay Inlet	0.96	595	1613	20
West Bay Inlet	0.84	1007	1784	203
West Bay – A2	0.97	369	740	65
West Seapuit	0.83	99	156	9
East Seapuit	0.94	114	212	2

V.4.2.6 Model Circulation Characteristics

The final calibrated model serves as a useful tool in investigating the circulation characteristics of the Three Bays system. Using model inputs of bathymetry and tide data, current velocities and flow rates can be determined at any point in the model domain. This is a very useful feature of a hydrodynamic model, where a limited amount of collected data can be expanded to determine the physical attributes of the system in areas where no physical data record exists.

From the model run of the Three Bays system, maximum ebb velocities in the inlet channels are slightly larger than velocities during maximum flood. Maximum depth-averaged flood velocities in the model are approximately 1.5 feet/sec at West Bay Inlet and 1.1 ft sec at Cotuit Bay inlet, while maximum ebb velocities are about 2.1 feet/sec at West Bay inlet and 1.7 ft/sec at Cotuit Bay Inlet. At both the Little Island Bridge and the Cotuit Bay entrance to North Bay, typical peak flood and ebb velocities are 0.8 ft/sec and 1.1 ft/sec, respectively. Close-up views of model output are presented in Figure V-37 and V-38, which show contours of velocity magnitude along with velocity vectors that indicate flow direction, each for a single model time-step, at the portion of the tide where maximum ebb velocities occur (in Figure V-37), and for maximum flood velocities in Figure V-38.

In addition to depth-averaged velocities, the total flow rate of water flowing through a channel can be computed with the hydrodynamic model. For the flushing analysis in the next section, flow rates were computed across 12 separate transects in the Three Bays system. The variation of flow as the tide floods and ebbs at the two system inlets is seen in the plot of flow rates in Figure V-39. Maximum flow rates occur during ebbing tides in this system. During spring tides, the maximum flood flow rates reach 4500 ft^3/sec at West Bay Inlet. Maximum ebb flow rates during spring tides are slightly greater at West Bay Inlet, about 6800 ft^3/sec. Minimum flood flows at West Bay Inlet during neap tides are 3300 ft^3/sec, and minimum ebb flows during neap tides are approximately 4300 ft^3/sec. The flow magnitudes through Cotuit Inlet are typically 10% less than the flows through West Bay Inlet.

The model is useful to demonstrate some of the unique hydrodynamic traits of the Three Bays system. The Seapuit River, for example, is a rare feature among estuaries in general. It is connected at both ends to separate embayments, which in turn have their own inlets to the ocean. It would be difficult to define the upstream and downstream portions of this tidal river based only on its geographical characteristics. However, ADCP measurements, and model results show that there is a definite “downstream” flow direction. Flow through the Seapuit River is driven by the time difference (lag) of the tide stage between Cotuit Inlet and West Bay Inlet. When the tide is flooding, the river will flow from east to west (the “upstream” direction), and *vice versa* for an ebbing tide. Both model and measurements show that peak flows at the west end of the river are less than peak flows at the east end. At first, this result may seem problematic,

as a violation of mass conservation. The expectation is that for a river without additional tributary input, flow across any cross-stream transect should be the same. However, for the Seapuit River, a large portion of the flow into the river during a flooding tide does not exit the other end because it stays within the river basin, resulting in an increase in water elevation. Integrating the flow curves over a half tide cycle (e.g., from slack low to slack high tide) and subtracting the total flow though the west transect from the total flow trough the east transect results in the total tide prism between the two transects (i.e., the tide prism of the Seapuit River). This can be expressed as

$$V_{prism} = \int \left[\left(\frac{dV}{dt} \right)_{east} - \left(\frac{dV}{dt} \right)_{west} \right] dt$$

where V_{prism} is the prism volume, and dV/dt is the volume flow rate across the indicated transect. During the ADCP survey time period, the tide prism is computed to be about 3.6×10^6 cubic feet.

Another feature of the Three Bays system model is a persistent tidal eddy (or gyre) in Cotuit Bay, which is set-up during flooding tides. The eddy can be seen in model output shown in Figure V-40, to the north of Bluff Point in Cotuit. The eddy has a faint counter-clock-wise rotation, with velocity magnitudes that are less than 0.2 ft/sec.

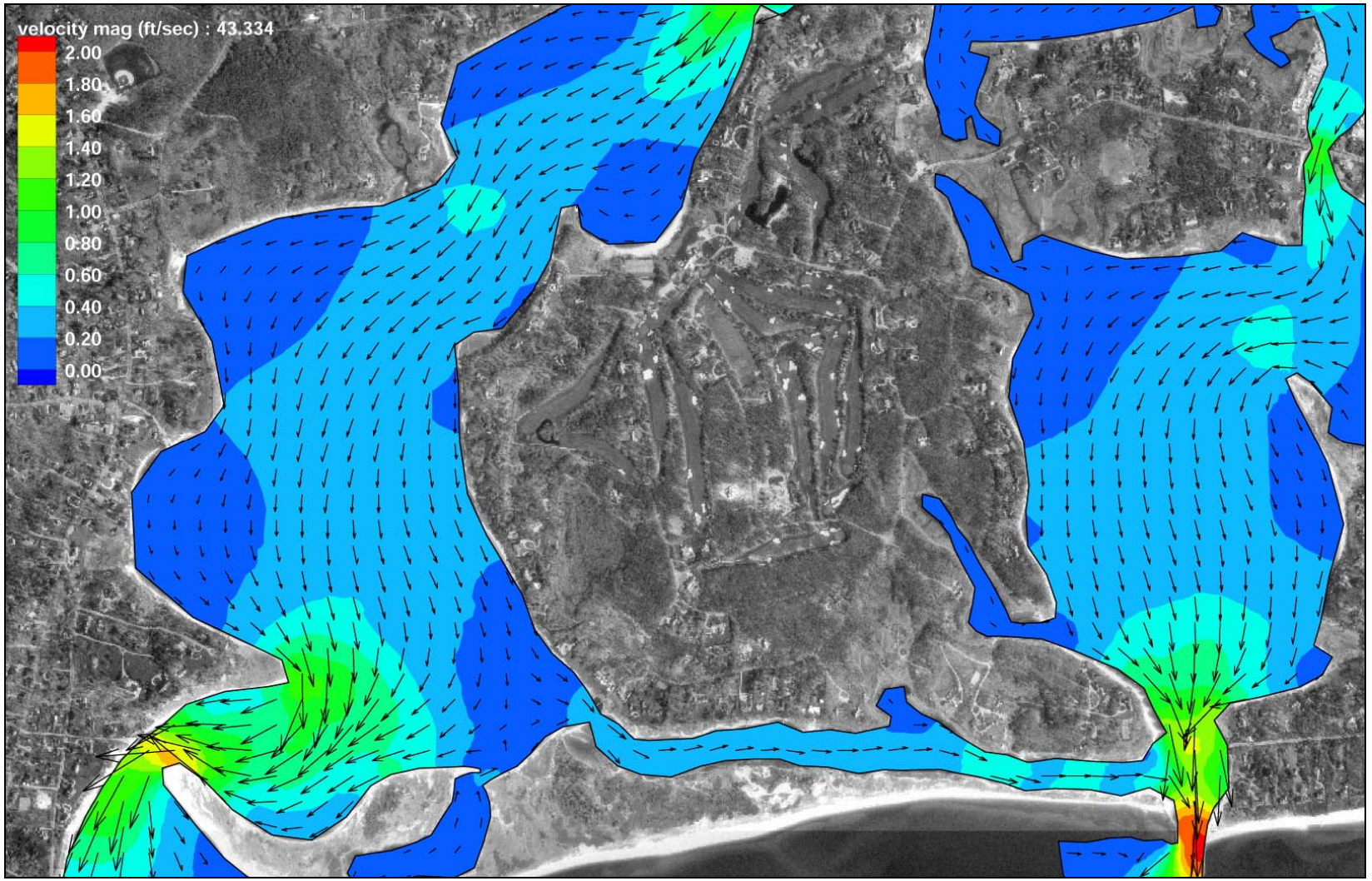

Figure V-37. Example of hydrodynamic model output for a single time step where maximum ebb velocities occur for this tide cycle. Color contours indicate velocity magnitude, and vectors indicate the direction of flow.

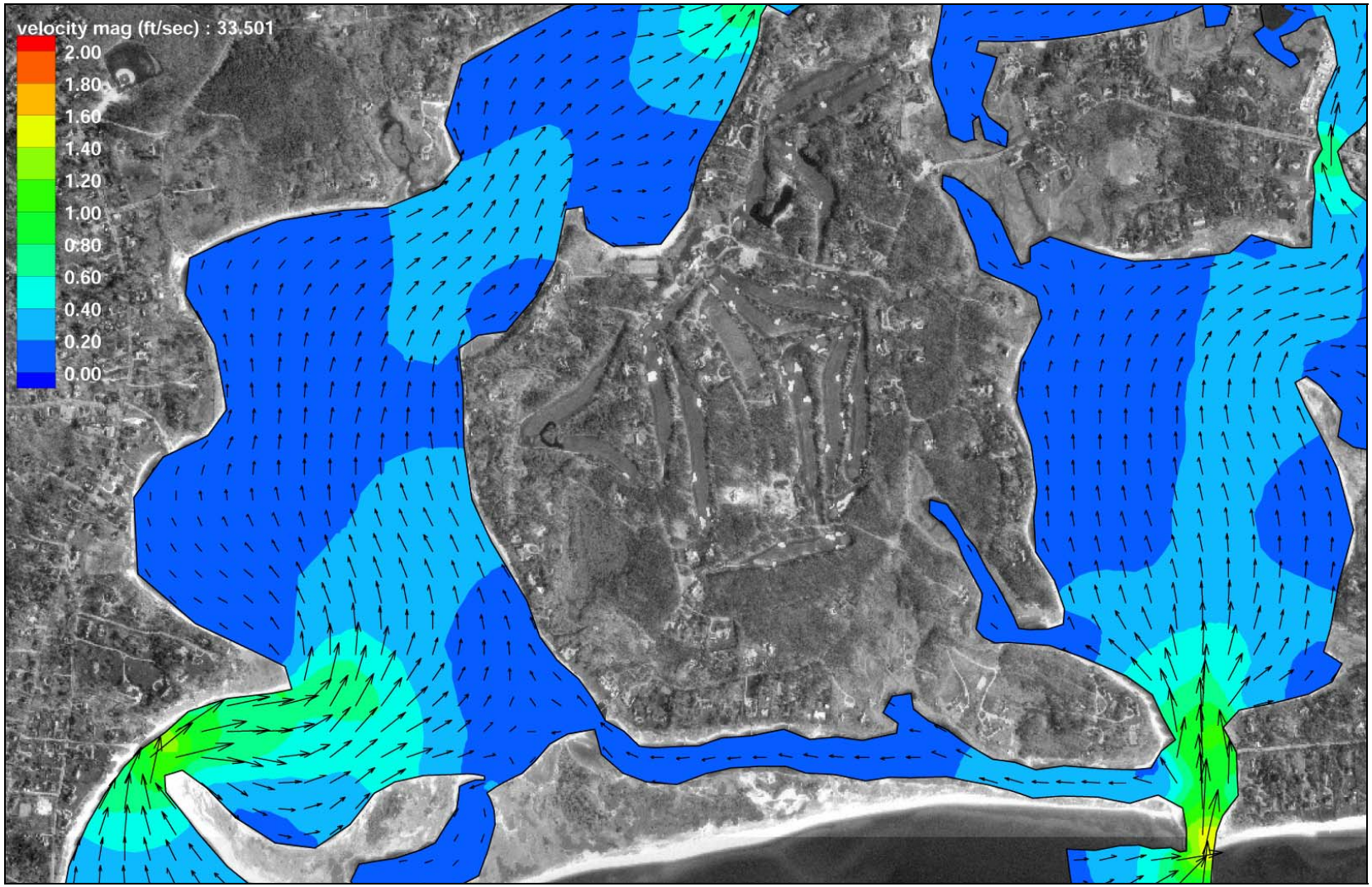

Figure V-38. Example of hydrodynamic model output for a single time step where maximum ebb velocities occur for this tide cycle. Color contours indicate velocity magnitude, and vectors indicate the direction of flow.

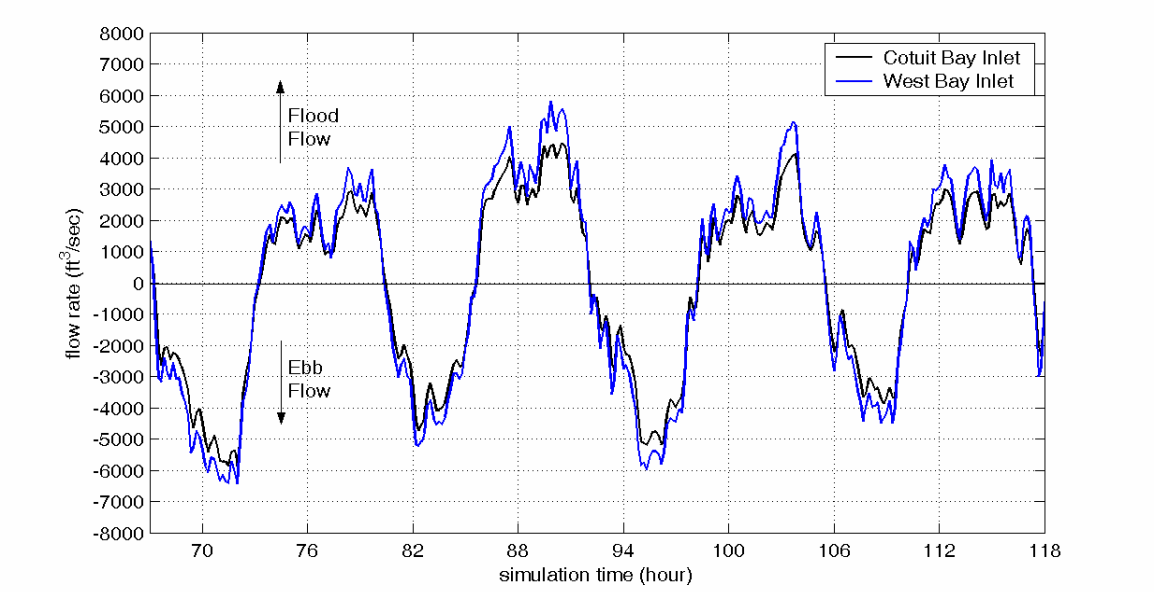

Figure V-39. Time variation of computed flow rates for the two inlets of the Three Bays system. . Plotted time period represents four tide cycles (12.42 h cycle). Positive flow indicated flooding tide, while negative flow indicates ebbing tide.

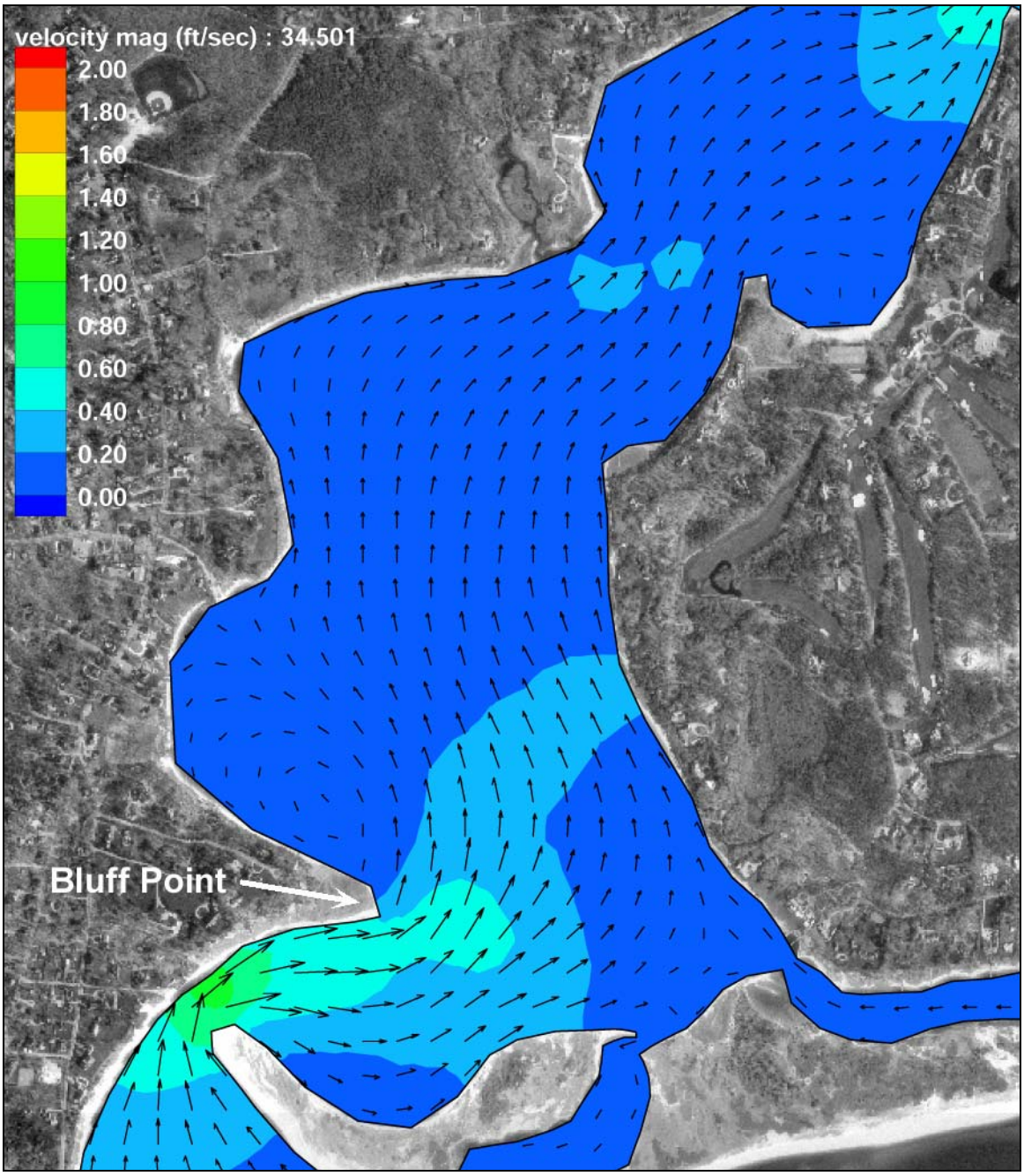

Figure V-40. Close-up of Cotuit Bay, showing output from the Three Bays hydrodynamic model at a single time step, where a recirculation eddy (or gyre) has set up on the north side of Bluff Point.

V.5 FLUSHING CHARACTERISTICS

Since the magnitude of freshwater inflow is much smaller in comparison to the tidal exchange through each inlet, the primary mechanism controlling estuarine water quality within the modeled Three Bays system is tidal exchange. A rising tide offshore in Nantucket Sound creates a slope in water surface from the ocean into the modeled systems. Consequently, water flows into (floods) the system. Similarly, the estuary drains into the open waters of Nantucket Sound on an ebbing tide. This exchange of water between the system and the

ocean is defined as tidal flushing. The calibrated hydrodynamic model is a tool to evaluate quantitatively tidal flushing of the Three Bays system, and was used to compute flushing rates (residence times) and tidal circulation patterns.

Flushing rate, or residence time, is defined as the average time required for a parcel of water to migrate out of an estuary from points within the system. For this study, **system residence times** were computed as the average time required for a water parcel to migrate from a point within the each embayment to the entrance of the system. System residence times are computed as follows:

$$T_{system} = \frac{V_{system}}{P} t_{cycle}$$

where T_{system} denotes the residence time for the system, V_{system} represents volume of the (entire) system at mean tide level, P equals the tidal prism (or volume entering the system through a single tidal cycle), and t_{cycle} the period of the tidal cycle, typically 12.42 hours (or 0.52 days). To compute system residence time for a sub-embayment, the tidal prism of the sub-embayment replaces the total system tidal prism value in the above equation.

In addition to system residence times, a second residence, the **local residence time**, was defined as the average time required for a water parcel to migrate from a location within a sub-embayment to a point outside the sub-embayment. Using Dam Pond as an example, the **system residence time** is the average time required for water to migrate from Dam Pond, through North Bay, out through West Bay or Cotuit Bay, and into Nantucket Sound, where the **local residence time** is the average time required for water to migrate from Dam Pond to just North Bay (not all the way to the Sound). Local residence times for each sub-embayment are computed as:

$$T_{local} = \frac{V_{local}}{P} t_{cycle}$$

where T_{local} denotes the residence time for the local sub-embayment, V_{local} represents the volume of the sub-embayment at mean tide level, P equals the tidal prism (or volume entering the local sub-embayment through a single tidal cycle), and t_{cycle} the period of the tidal cycle (again, 0.52 days).

Residence times are provided as a first order evaluation of estuarine water quality. Lower residence times generally correspond to higher water quality; however, residence times may be misleading depending upon pollutant/nutrient loading rates and the overall quality of the receiving waters. As a qualitative guide, **system residence times** are applicable for systems where the water quality within the entire estuary is degraded and higher quality waters provide the only means of reducing the high nutrient levels. For the Three Bays system this approach is applicable, since it assumes the main system has relatively lower quality water relative to Nantucket Sound.

The rate of pollutant/nutrient loading and the quality of water outside the estuary both must be evaluated in conjunction with residence times to obtain a clear picture of water quality. It is impossible to evaluate an estuary's health based solely on flushing rates. Efficient tidal flushing (low residence time) is not an indication of high water quality if pollutants and nutrients are loaded into the estuary faster than the tidal circulation can flush the system. Neither are low

residence times an indicator of high water quality if the water flushed into the estuary is of poor quality. Advanced understanding of water quality will be obtained from the calibrated hydrodynamic model by extending the model to include pollutant/nutrient dispersion. The water quality model will provide a valuable tool to evaluate the complex mechanisms governing estuarine water quality in the Three Bays system.

Since the calibrated RMA-2 model simulated accurate two-dimensional hydrodynamics in the system, model results were used to compute residence times. Residence times were computed for the entire estuary, as well the six sub-embayments within the system. In addition, **system** and **local residence times** were computed to indicate the range of conditions possible for the system.

Residence times were calculated as the volume of water (based on the mean volumes computed for the simulation period) in the entire system divided by the average volume of water exchanged with each sub-embayment over a flood tidal cycle (tidal prism). Units then were converted to days. The volume of the entire estuary was computed as cubic feet. Model divisions used to define the system sub-embayments include 1) the entire Three Bays system, 2) North Bay, including the Marstons Mills River, Prince's Cove and Warren's Cove, 3) the Marstons Mills River with Prince's Cove and Warren's Cove, 4) Prince's Cove, 5) Warren's Cove, 6) Dam Pond, and 7) Eel River. These system divisions follow the model material type areas designated in Figure V-24. Sub-embayment mean volumes and tide prisms are presented in Table V-9.

Residence times were averaged for the tidal cycles comprising a representative 7 lunar day period (14 tide cycles), and are listed in Table V-10. The modeled time period used to compute the flushing rates was that same as the model verification period, and included the transition from neap to spring tide conditions. The RMA-2 model calculated flow crossing specified grid lines for each sub-embayment to compute the tidal prism volume. Since the 7 lunar day period used to compute the flushing rates of the system represent average tidal conditions, the measurements provide the most appropriate method for determining mean flushing rates for the system sub-embayments.

Table V-9. Embayment mean volumes and average tidal prism during simulation period.

Embayment	Mean Volume (ft^3)	Tide Prism Volume (ft^3)
Three Bays System	429,117,000	140,570,000
North Bay	139,666,000	45,824,000
Marstons Mills River	25,236,000	10,834,000
Prince's Cove	13,007,000	4,553,000
Warren's Cove	5,047,000	3,614,000
Dam Pond	2,798,000	1,200,000
Eel River	4,035,000	1,702,000

Table V-10. Computed System and Local residence times for embayments in the Three Bays system.

Embayment	System Residence Time (days)	Local Residence Time (days)
Three Bays System	1.6	1.6
North Bay	4.8	1.6
Marstons Mills River	20.5	1.2
Prince's Cove	48.8	1.5
Warren's Cove	61.4	0.7
Dam Pond	185.1	1.2
Eel River	130.5	1.2

The computed flushing rates for the Three Bays system show that as a whole, the system flushes well. A flushing time of 1.6 days for the entire estuary shows that on average, water is resident in the system less than two days. All system sub-embayments have local flushing times that are equal to or less than 2 days. Warren's Cove has the shortest local flushing time, because of its small mean sub-embayment volume, relative to its tide prism.

The low local residence times in all areas of the Three Bays system show that they would likely have good water quality if the system water with which it exchanges also has good water quality. For example, the water quality of Eel River would likely be good as long as the water quality of West Bay was also good. Actual water quality would still also depend upon the total nutrient load to each embayment.

For the smaller sub-embayments of the Three Bays system, computed system residence times are typically one or two orders of magnitude longer than their corresponding local residence time. System residence times provide a qualitative measure that helps to identify the relative sensitivity of different sub-embayments to nutrient loading.

Based on our knowledge of estuarine processes, we estimate that the combined errors associated with the method applied to compute residence times are within 10% to 15% of "true" residence times, for the Three Bays system. Possible errors in computed residence times can be linked to two sources: the bathymetry information and simplifications employed to calculate residence time. In this study, the most significant errors associated with the bathymetry data result from the process of interpolating the data to the finite element mesh, which was the basis for all the flushing volumes used in the analysis. In addition, limited topographic measurements were available in some of the smaller sub-embayments of the system.

Minor errors may be introduced in residence time calculations by simplifying assumptions. Flushing rate calculations assume that water exiting an estuary or sub-embayment does not return on the following tidal cycle. For regions where a strong littoral drift exists, this assumption is valid. However, water exiting a small sub-embayment on a relatively calm day may not completely mix with estuarine waters. In this case, the "strong littoral drift" assumption would lead to an under-prediction of residence time. Since littoral drift along the shoreline of Nantucket Sound typically is strong because of the effects of the local winds and tidal induced mixing within Nantucket Sound, the "strong littoral drift" assumption only will cause minor errors in residence time calculations.